DEPARTMENT OF TRANSPORTATION

Value of Dedicated Right-of-Way: Transit Service Reliability and User Impacts

Ying Song, Principal Investigator
Geography, Environment, and Society
University of Minnesota

February 2025

Research Report
Final Report 2025-01

To get this document in an alternative format or language, please call 651-366-4720 (711 or 1-800-627-3529 for MN Relay). You can also email your request to ADArequest.dot@state.mn.us. Please make your request at least two weeks before you need the document.

Technical Report Documentation Page

1. Report No.	2.	3. Recipients Accession No.
MN 2025-01		

4. Title and Subtitle	5. Report Date
Value of Dedicated Right-of-Way: Transit Service Reliability and User Impacts	February 2025
	6.

7. Author(s)	8. Performing Organization Report No.
Ying Song, Xiaohuan Zeng, Alireza Khani, Sahas Sok	

9. Performing Organization Name and Address	10. Project/Task/Work Unit No.
Geography, Environment, and Society University of Minnesota – Twin Cities 414 Social Science Building, 267 19th Ave S, Minneapolis, MN 55455	#2024015
	11. Contract (C) or Grant (G) No. (c) 1036342 (wo) 95

12. Sponsoring Organization Name and Address	13. Type of Report and Period Covered
Minnesota Department of Transportation Office of Research & Innovation 395 John Ireland Boulevard, MS 330 St. Paul, Minnesota 55155-1899	Final Report
	14. Sponsoring Agency Code

15. Supplementary Notes

http://mdl.mndot.gov/

16. Abstract (229 words)

Transit services connect people to jobs and opportunities, fostering vibrant communities and multimodal travel along service corridors. A transit right-of-way (ROW) can help buses bypass congestion and stay on schedule. Many studies have proved that transit ROWs effectively improve service reliability and reduce user costs. However, these studies often focus on one or two service corridors, limiting comprehensive impact assessment. This project addresses this gap by investigating service reliability for all route segments across a transit system.

We derived reliability metrics at the route segment level using high-resolution automatic vehicle location (AVL) and automatic passenger count (APC) data collected in the Twin Cities metropolitan area. We then collected and integrated data from various sources via spatial-temporal computing to capture service characteristics, operating environments, traffic conditions, and land-use features along route segments. We applied the Gradient Boosting Model (GBM) to examine nonlinear relationships between these factors and bus travel time reliability. Lastly, we used the trained model to estimate potential improvements in reliability with dedicated ROWs. Through these steps, we worked with members of the Technical Advisory Panel (TAP) to illustrate our methodology and demonstrate its utility for transit agencies. Specifically, the results proved that the ratio of bus lanes and busways was associated with more reliable travel time along route segments. We also found that route segments along a few service corridors with unreliable services can greatly benefit from implementing a dedicated ROW.

17. Document Analysis/Descriptors	18. Availability Statement
Dedicated right-of-way, transit service reliability, gradient boosting model (GBM), automatic vehicle location (AVL), automatic passenger count (APC)	No restrictions. Document available from: National Technical Information Services, Alexandria, Virginia 22312

19. Security Class (this report)	20. Security Class (this page)	21. No. of Pages	22. Price
Unclassified	Unclassified	55	

Value of Dedicated Right-of-Way: Transit Service Reliability and User Impacts

Final Report

Prepared by:

Ying Song
Xiaohuan Zeng
Department of Geography, Environment, and Society
University of Minnesota – Twin Cities

Alireza Khani
Sahas Sok
Civil, Environmental, and Geo- Engineering
University of Minnesota – Twin Cities

February 2025

Published by:

Minnesota Department of Transportation
Office of Research & Innovation
395 John Ireland Boulevard, MS 330
St. Paul, Minnesota 55155-1899

ACKNOWLEDGMENTS

The research team would like to acknowledge the members of this project's Technical Advisory Panel (TAP) for their assistance throughout the project development and report review.

Members of the TAP include:

(Current and past technical liaisons)

Amrish Patel, Metro District, MnDOT

Sarah Ghandour, Transit and Active Transportation, MnDOT

Edward Sanderson, Metro District, MnDOT

Kimberly Zlimen, Metro District, MnDOT

(Project coordinator)

Barbara Fraley, Research and Innovation, MnDOT

(Panel member)

Jennifer Jordan, Ramsey County

Eric Lind, Accessibility Observatory, University of Minnesota

Emma Lucken, Ramsey County

Mike Mechtenberg, Metro Transit

Joey Reid, Metro Transit

Aaron Tag, Metro District, MnDOT

Ophelia Washington, Ramsey County

Maxwell Wilson, Hennepin County

Marcus Bekele, Research and Innovation, MnDOT

(Communication adviser)

Micaela Kranz, Research and Innovation

Table of Contents

List of Figures

List of Tables

LIST OF ABBREVIATIONS

AFC – Automatic Fare Collection

APC – Automatic Passenger Count

AVL – Automatic Vehicle Location

BRT – Bus Rapid Transit

GBM – Gradient Boosting Model

MAD – Median Absolute Deviation

ROW – Right of Way

TAP – Technical Advisory Panel

EXECUTIVE SUMMARY

In urban areas with dense and mixed land use and high traffic, transit service provides a sustainable way to connect people to jobs and opportunities and creates vibrant areas around serviced corridors. Transit service reliability is often among the most requested service improvements and plays a significant role in reducing travel costs, increasing ridership, and attracting and retaining users. Recent studies have used automatic vehicle location (AVL), automated passenger count (APC), and other automatic data to derive reliability measures. However, only some studies have explicitly investigated the impacts of dedicated right-of-way (ROW) on service reliability using these datasets.

To address this gap, this research project examined how service reliability varied across route segments in the transit system and what factors were strongly associated with low/high service reliability. First, we used the AVL and APC data to calculate the running time variability and used it to evaluate reliability for each route segment between two stops. We then collected and integrated data from multiple sources to capture factors affecting bus travel time variability, such as the free flow speed, traffic volumes, and the presence of ROWs. Next, we associated these factors with service reliability along route segments using the Gradient Boosting Model (GBM). We chose GBM because this machine-learning method can handle highly correlated input variables and provide interpretable learning outcomes. Lastly, we used the trained model to estimate potential improvements in reliability after implementing dedicated ROW and identify route segments with the greatest estimated improvement across the system. The research team worked with members of the Technical Advisory Panel (TAP) throughout the process to ensure the input data sources, model settings, and result interpretations were interpretable and aligned with real-world practices.

Explorations of the median and variability of bus travel times showed that 1) segments along suburban local routes generally had the best performance, likely due to the relatively light traffic in the suburban areas, 2) segments along commuter express routes had the least reliable travel times potential due to their operating time during morning and afternoon peak hours as well as heavy traffic during these commuting routes, and 3) compared to urban local routes, segments along BRT routes had slightly faster and more reliable services even with more frequent services and higher ridership, which was potentially due to the operating environment along BRT routes as well as stop designs.

Model training outcomes suggested that the ratio of bus lanes and busways along a route segment was associated with decreased travel time variability and, hence, more reliable service; the presence of HOV and HOT was associated with improved reliability, but a higher ratio of HOV and HOT was not associated with a greater improvement; and the presence of shoulder lanes did not help much with reliability. Besides various types of transit ROWs, the model revealed that higher free-flow speeds, fewer traffic signals, and longer segments were the three top-ranking factors associated with more reliable service. In addition, we found that factors may interact with each other while contributing to the travel time variability. Specifically, more traffic lights along route segments may lead to less reliable travel time,

even with dedicated ROWs. This suggested that future design and implementation of dedicated ROWs need to consider other factors, such as signal priority, to maximize their benefits.

Model estimations of reliability revealed route segments along several service corridors that may greatly benefit from bus lanes and busways. Specifically, we compared MADs and user-weighted MADs for each route segment with and without bus lanes and busways and identified segments with higher reductions in MAD. We then examined other routes operating along or across the same corridor to provide a more comprehensive evaluation of the benefits of implementing bus lanes and busways. The results revealed several corridors with the greatest benefits, including 1) Route 21 along Lake Street, 2) Routes 4 and 10 10 along Hennepin Ave crossing the bridge, and 3) Routes 5 and 14 along South 7th Street and South 8th Street.

In sum, the project tackled crucial and timely questions in public transportation studies from different angles by evaluating service reliability at the route segment level, identifying key factors contributing to high reliability, and estimating potential improvements in reliability after implementing dedicated ROWs along each route segment. The outcomes can lead to informed decisions about funding future projects, such as prioritizing and implementing bus lanes along service corridors with high potential benefits.

Chapter 1: Introduction

Transit service provides a sustainable way to connect people to jobs and opportunities, fostering vibrant communities near service corridors (Far 2011, Suzuki et al. 2013). Reliable transit services play a crucial role in attracting and retaining users (Perk et al., 2008; Van Lierop, 2018), increasing ridership (Berrebi et al., 2022; Taylor & Fink, 2003), and reducing travel costs (Casello et al., 2009; Wright & Hook, 2007). Recent studies on bus rapid transit (BRT) impacts also demonstrate the positive effects of reliable transit services on ridership, housing values, and job access along service routes (Benson & Cao, 2020; Guthrie & Fan, 2016; Acton et al., 2022).

A transit right-of-way (ROW) allows transit vehicles to bypass congestion, helps vehicles stay on schedule, and moves people more quickly through congested corridors (APTA, 2010; Levinson et al., 2002; City of Minneapolis, 2023). Empirical studies have proven that the implementation of a transit ROW can improve headway adherence (Tirachini et al. 2022, González et al. 2018), reduce the impacts of traffic congestion on bus travel time (Sakamoto et al. 2007, Othman et al. 2023), and boost the ridership (Ko et al. 2019, Cao et al. 2023). However, most studies focus on the system-level or route-level analysis and do not examine how the impact of dedicated ROWs may vary across routes and segments in the transit system.

This project aims to address this gap by examining the values of dedicated ROWs regarding improving service reliability and reducing user travel costs at the route segment level. The specific aims of this research include:

- *Examine how service reliability varies across transitways and service corridors*. The project will use automatic vehicle location (AVL) and automated passenger count (APC) data to calculate reliability indices along route segments between two consecutive stops along service routes.
- *Investigate what factors are strongly associated with low/high service reliability*. The project will examine associations between the reliability indices and the presence of transit ROWs while accounting for other potential factors, such as mixed traffic and service frequencies.
- *Evaluate the benefits of transit ROWs regarding improved reliability and reduced user costs*. The project will use the revealed relationship between reliability indices and contributing factors to assess potential improvements in service reliability and the consequent user benefits.

This report is organized as follows: Chapter 2 briefly reviews transit service reliability metrics from both agency and user perspectives; Chapter 3 presents the research design with procedures and methods to answer the three research questions; Chapter 4 summarizes data collection and integration outcomes; Chapter 5 presents model training results and discusses their implications; and finally, Chapter 6 provides a summary and conclusions.

Chapter 2: Transit Service Reliability

This chapter summarizes transit service reliability measures. We used the Transit Cooperative Research Program (TCRP) Research Report 215: "Minutes Matter: A Bus Transit Service Reliability Guidebook" as the primary reference (Danaher et al., 2020) and included a few recent publications.

2.1 Three Aspects of Reliability

The increasing availability of automatic vehicle location (AVL) data and automatic passenger count (APC) data allows transit agencies and researchers to define and evaluate service reliability using finer-grained and data-intensive methods. Despite various definitions of service reliability, they commonly address at least one of the following three aspects of reliability:

- **Punctuality** refers to whether and how well a bus service sticks to its published schedule. Reliability measures concerning punctuality are defined by comparing the actual arrival or departure times at stops with the schedule or expected time. For instance, if the schedule suggests the bus will serve at a stop at 8:00 am, arriving at the stop at 8:02 am, 8:10 am, and 8:15 am would mean different levels of service reliability.
- **Variability** refers to whether and to which degree a bus service can provide consistent service over time. For instance, constantly arriving at a stop about 3 minutes late has a lower level of variability and a higher reliability level than arriving late at a stop for 3 minutes one day, 10 minutes the next day, and 15 minutes the day afterward.
- **Non-operation** refers to whether a bus service is available as it should be. For instance, if a trip fails to run due to vehicle mechanical issues, it will lead to non-operational reliability issues.

2.2 Four Levels of Reliability

The transit service reliability can be evaluated at the following four different levels:

- **System-level** measures are calculated for all services a transit agency provides (or all services of a specific service type). These measures provide an overall performance assessment and are usually used in summary reports to be shared with the public and stakeholders.
- **Route-level** measures are calculated separately for each route in a specific system, which can be used to identify routes with less reliable services that may need more attention.
- **Trip-level** measures are calculated separately for each trip along a specific route over multiple days, which can be used to identify trip(s) with less reliable services and inform strategies such as updates on transit schedules (to improve punctuality) and signal priority (to reduce variability).

- **Stop-level** measures are calculated based on recorded data at each stop along a route over multiple trips. They can be used to examine spatial variations of reliability along a route and identify parts of the route with the least reliable services

2.3 Common Reliability Measures

This subsection summarizes frequently used reliability measures. Table 2.1 summarizes these measures. The rest of this subsection describes input data, calculation, analysis, and typical usage for each measure associated with bus travel time within the system.[1]

Table 2.1 Frequently used reliability measures (modified from Danaher et al. 2020)

Reliability Aspect	Data Needed	Measure	Level	Perspective
Punctuality	Arrival and departure times	On-time performance (schedule adherence)	All	All
Variability (travel time)	Trip start and end times	Running time	Route	Agency
	Dwell time at stops	Dwell time	Stop	Agency
	Passenger travel times	Travel time	System	Passenger
		Buffer time index	System	Passenger
Variability (wait time)	Time between buses	Headway	Route	Agency
	Passenger wait times	Wait time	System	Passenger
Non-operation	Missed service	Pullouts missed	System	Operator
		Missed hours of service	System	Operator
		Scheduled trips cancelled	System	Operator
	Service disruptions	Number of crashes	System	Operator
		Mean distance between failures	System	Operator
Multiple	Customer surveys	Passenger ratings of reliability		All

- **On-time performance** is evaluated by comparing actual and scheduled arrival and departure times, typically at time points, each with an explicitly scheduled arrival or departure time.
  - Agency often defines their specific on-time window during which a bus is neither late nor early. The most common window is zero or one minute early to five minutes late. Then, agencies use the percentage of stop arrivals falling within this window during a specific period to evaluate the overall on-time performance of a particular trip, route, or system.
  - Alternatively, the deviation of differences between actual and scheduled times at each stop can be computed using data collected during specific periods. Comparing deviations across all stops

[1] We do not include descriptions of no-operation variability given this project's focus on the values of dedicated right-of-way regarding travel time reliability.

along a particular route and throughout the system can reveal locations with less reliable services. Comparing deviations across different periods can reveal times with lower reliability.

On-time performance measures are straightforward and align well with our expectations of reliable transit services. Therefore, they are widely used for public and internal reporting. However, they do not effectively reveal the underlying causes of unreliable services.

- **Running time variability** is evaluated using the recorded bus travel time over the entire route or for route segments. The variability can be calculated using bus travel time for all trips or trips during a particular time of day. Typical measures include 1) variations (e.g., standard deviation, coefficient of variation), 2) extreme delays (e.g., 95th percentile divided by the mean), and 3) reliable ranges (e.g., the percentage within a specific absolute or relative range). The variability measure of running times emphasizes the consistency in bus travel time. Therefore, transit agencies have widely used it to compare performances across service routes (or route segments) and inform future adjustments in service schedules or improvements in route designs and operations.
- **Dwelling time variability** is evaluated using the recorded time spent at bus stops for a specific time of day from either APC data or manual observations. The dwelling time variability can be calculated using similar approaches to the running time variability. The measured variability can be used in the statistical model to understand whether the variability is related only to the number of boarding and alighting passengers or high loads of onboard passengers. Agencies commonly use this measure to narrow down potential causes of unreliability at the stop level.
- **Passenger travel time variability** is evaluated through three main steps. First, the ridership for each possible O/D pair is estimated via travel demand modeling and simulations using a combination of data such as Automatic Fare Collection (AFC), APC, and transit onboard O/D survey data. Second, AVL data are used to estimate the travel time variability for each O/D pair during a period, which is computationally expensive, especially for O/D pairs requiring transfers. Last, the variabilities of all O/D pairs are weighted by the corresponding ridership and summed up for the entire system. While providing a rich depiction of reliability as experienced by the passenger, this measure is not practical for identifying improvement strategies.
- **Passenger buffer time index** is evaluated using the same data as passenger travel time variability. First, O/D ridership patterns are estimated using AFC, APC, and survey data. Second, the buffer time for each possible O/D pair is calculated using the 95^{th} percentile of passenger travel times estimated using AVL data. Last, the variation of buffer time indices across all O/D pairs is used to evaluate the system-level variability. Like the passenger travel time variability, this measure is not practical.
- **Headway variability** is measured based on the time between consecutive trips at each stop along a route or corridor. The variability is calculated for a route during the period over which the scheduled headway is constant. The calculation uses methods like those used for the running time variability. Agencies commonly use this measure to identify routes with unsatisfactory variabilities, especially those with headway intervals of less than 10 or 15 minutes.

- **Passenger wait time variability** is estimated based on headways at stops along a route and ridership by trip obtained from AVL/APC/AFC data. With random arrivals of passengers on service routes with short scheduled headways, the average wait time for each observed trip is assumed to be half of the observed headway. Excess wait time per passenger at each stop can be measured by subtracting the expected wait time based on the scheduled headway from the observed wait time. The variability of excess wait time across the system is calculated using methods like those used for the running time variability (e.g., coefficient of variation).
- **Passenger rating of reliability** is evaluated using data collected through onboard surveys, telephone or online surveys, social media platforms, and public meetings. These surveys are often designed to address the overall travel experience or specific elements of service reliability, such as waiting time. The overall reliability ratings can be calculated as the percentage of responses within a given range. The passenger reliability rating recognizes that passengers' perceptions of reliability primarily affect their travel choices and experiences and, hence, can provide insights into how customers perceive treatments and may potentially affect ridership.

Based on the review of frequently used reliability measures, this project chooses to use the running time variability considering that such measure 1) can evaluate reliability at the route segment level and reveal spatial variation along routes and across the entire system, 2) does not require transit schedules as data inputs which are only available at the time points, 3) has already been widely applied by transit agencies in performance evaluation, and 4) is possible to integrate into statistical models that relate the reliability outcome to potential contributing factors such as the service type and operating environment. We also learned from passenger travel time variability. We calculated user-weighted running time variability to estimate the benefits of transit ROW in terms of reduced user travel costs along route segments.

Chapter 3: Research Design

This chapter presents the research design with procedures and methods to measure service reliability at the route segment level and identify critical factors contributing to the least/most reliable services.

3.1 Framework

Figure 3.1 illustrates the research design with three key components: 1) pre-modeling data exploration, 2) model training and fine-tuning, and 3) post-modeling result interpretation. During these processes, the research team collected feedback from members of the technical advisory board (TAP) regarding parameters, data, model settings, and result illustrations and used them to revise the model.

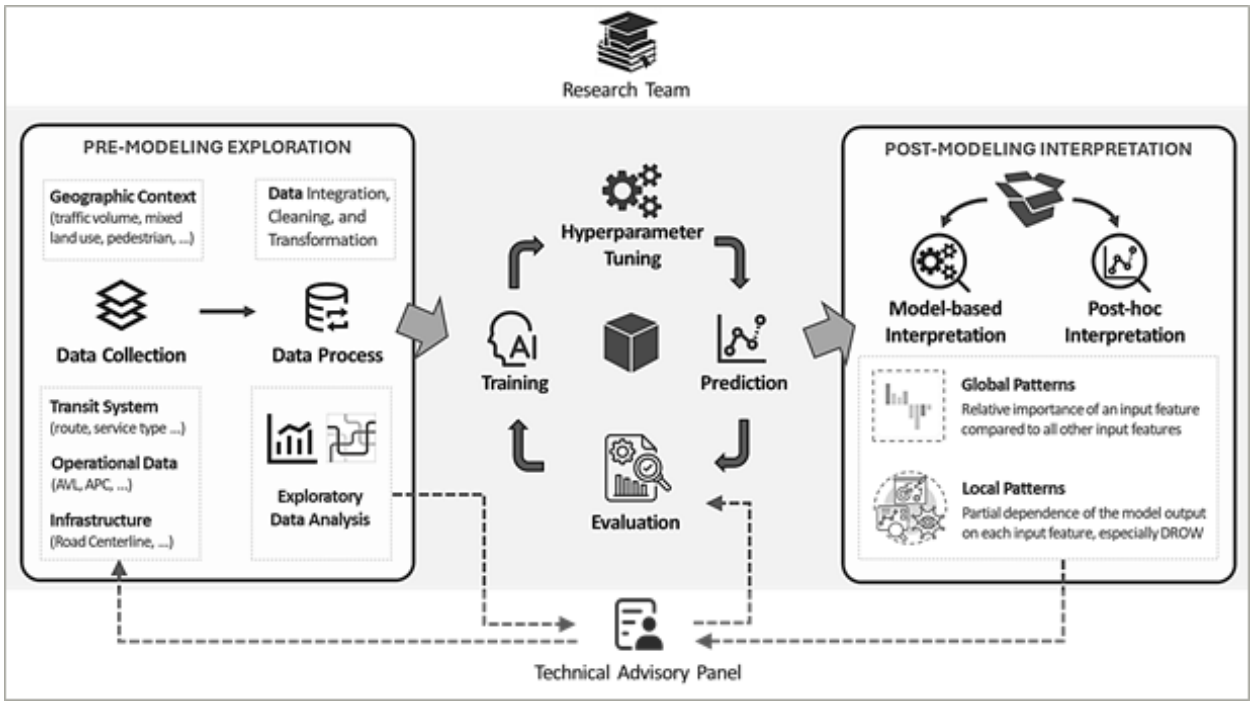

Figure 3.1 Research design with three key components

3.2 Data Collection

We collected and managed data for factors that may be strongly associated with running time variability besides the AVL and APC data. This subsection summarizes data sources used to derive these factors.

- **Street Centerline**[2]**:** The dataset was created through a collaborative project with ten metropolitan counties, the Metropolitan Emergency Services Board, MetroGIS, and the Metropolitan Council. The dataset served as the base spatial transport network for our analysis.
- **Route Segments**: Metro Transit kindly provided the dataset, which contained spatial geometries of each route segment and its associated properties such as route ID, origin stop ID, destination stop ID, and operating period. The route segments' geometries matched with the street centerlines.
- **Transit Rights-of-Way Segments**[3]: This dataset stored road segments where transit vehicles were permitted to operate while mixed traffic was prohibited or had limited access to operate. The spatial geometry of segments was derived from the NCompass Technologies Street Centerline dataset. So, we map-matched these segments to the street centerlines to keep the spatial elements consistent across the dataset. Besides, our analysis only considered bus lanes, busways, HOT or HOV lanes, and shoulder lanes as the transit ROW types. Given our focus on bus movements along route segments, we did not consider commuter rail, light rail, meter bypasses, and online stations.
- **Traffic Signals**[4]: The traffic signals, also known as traffic lights, were retrieved from Open Street Map (OSM) using the tag for signaling devices positioned at road intersections with specified directions. The locations of traffic signals were map-matched to route segments to derive the number of signals along each route segment.
- **Roadway Lanes**[5]: The roadway lane datasets were maintained by the Minnesota Department of Transportation. These datasets store basic information about roadway lanes, including the number of through lanes and the width of the roadway carrying through traffic. The geometry of roadway lanes was map-matched to each route segment to derive roadway properties along that segment.
- **Parking Spaces**[6]: Designated parking spaces in downtown Minneapolis and St. Paul are provided by the cities of Minneapolis and St. Paul. The datasets stored locations of parking spaces in the cities, which were matched to route segments as one operating environment feature.
- **Traffic Conditions I**[7]: We retrieved traffic conditions along route segments from StreetLight, such as free-flow and median traffic speed and daily traffic volumes. No map matching was needed since the route segment geometry was used to retrieve the information.

---

[2] Road Centerlines (Geospatial Advisory Council Schema). Accessed Jul. 2023 at: https://gisdata.mn.gov/dataset/us-mn-state-metrogis-trans-road-centerlines-gac

[3] Transit Rights-of-Way Segments (Transit Advantages). Accessed Jul. 2023 at: https://gisdata.mn.gov/dataset/us-mn-state-metc-trans-transit-row-segments

[4] Open Street Map (OSM) documentation: https://wiki.openstreetmap.org/wiki/Key:traffic_signals:direction

[5] Roadway Lane information in Minnesota. Accessed Sep. 2024 at: https://gisdata.mn.gov/dataset/trans-lanes

[6] Parking meter map. Retrieved Sep. 2024 from: https://www.minneapolismn.gov/getting-around/parking-driving/street-parking-meters/parking-meters/parking-meter-map/ and https://www.stpaul.gov/parking-saint-paul

[7] StreetLight Data: Big Data for Mobility. Accessed Aug. 2023 at: https://www.streetlightdata.com/our-data/

- **Traffic Conditions II**[8]: Since StreetLight data were derived from multi-sourced, public mobility data, data were unavailable along busways where general traffic was prohibited. Therefore, we used the annual average daily traffic (AADT) along street segments provided by the Minnesota Department of Transportation as a complementary data source for the traffic condition.
- **Built Environment**[9]: We examined the adjacent land-use types and population densities near each route segment using the Smart Location Mapping data provided by the Environmental Protection Agency (EPA). We accounted for factors that can likely affect the traffic along the segment, such as pedestrian intersection density, mixed employment, and network density.
- **Weather Conditions**[10]: We reconciled historical records from the National Weather Service to obtain weather conditions during the study periods. We considered two factors with potential influence on the service reliability: 1) daily precipitations (snowfalls and snow depths) and 2) daily temperatures (extreme cold and hot days). Weather conditions did not vary significantly across the study area, so we only used them in exploratory data analysis.
- **AVL and APC data**: Metro Transit kindly provided the AVL and APC data. The AVL data was provided in the form of stop-crossing records, which recorded the actual times a bus arrived and departed a stop along a trip on a route. The original APC data contained eight tables to store operator, vehicle, date, time, trip, and stop information, and we selected a few fields for our analysis. The following subsection describes the APC and AVL data in more detail.

3.3 Data Integration and Cleaning

This section summarizes data integration and cleaning methods. We first integrate AVL and APC data to calculate running time variability along route segments. We then integrate other related data to create variables for our model.

3.3.1 AVL and APC Data

This project used APC and AVL data provided by Metro Transit from January 1, 2022, to April 30, 2023. We chose this period because 1) we preferred to use the most recent dataset that can capture traffic situations and transit operations after the outbreak of the COVID-19 pandemic, 2) we needed at least one year of data to capture seasonable variations of reliability performance, especially during the winter season, and 3) this project started on July 2023.

[8] Annual Average Daily Traffic Segments in Minnesota. Accessed Sep. 2024 at: https://gisdata.mn.gov/dataset/trans-aadt-traffic-segments
[9] EPA Smart Location Mapping. Accessed Jul. 2023 at: https://www.epa.gov/smartgrowth/smart-location-mapping
[10] National Weather Service. Past Weather Information for the Twin Cities. Accessed Sep. 2023 at: https://www.weather.gov/mpx/mspclimate

AVL Data: The original AVL dataset has 136,508,408 records. We selected the fields in Table 3.1 out of 28 fields. For inputs of our analysis, we included the served date, the actual arrival and departure times, the scheduled departure time, the first door opening time, the last door closing times at each stop of a served trip on a route, and two data quality indices. We also kept the fields storing the properties of that stop, including its identifier (ID), the service block ID and its order in that block, the name, direction, and type of its served route, and its longitude and latitude.

Table 3.1 Selected fields in Automatic Vehicle Location (AVL) data

Field Name	Description
SERVICE_ABBR	Service type
ROUTE_ABBR	Route abbreviation
ROUTE_DIRECTION_ABBR	Route direction
TRIP_ID	Trip ID
BLOCK_ABBR	Block ID
BLOCK_STOP_ORDER	Stop order in the block.
GEO_NODE_ABBR	Stop ID
LATITUDE	Latitude of the stop
LONGITUDE	Longitude of the stop
CALENDAR_DATE	Calendar Date
ACTUAL_ARRIVAL_TIME	Actual arrival time
ACTUAL_DEPARTURE_TIME	Actual departure time
SCHEDULED_TIME	Scheduled departure time
DOOR_OPEN_TIME	First door open time
DOOR_CLOSE_TIME	Last door close time
REPEATED	Flag for repeated order record
OOO	Flag for out-of-order record

APC Data. The original APC dataset consisted of eight tables to store operator, vehicle, date, time, trip, and stop information besides the passenger counts. The original table with passenger counts, namely FACT_APC, contained 135,383,587 records. We joined the FACT_APC table with tables DIM_STOP and DIM_TRIP_TM to get stop and trip information. We selected the fields in Table 3.2 that allowed us to match APC data to AVL data and derived passenger loads along route segments across trips.

Table 3.2 Selected fields in Automatic Passenger Count (APC) data

Table Name	Field Name	Description
FACT_APC	CALENDAR_DATE	calendar date
	BOARD	passenger boarding count
	ALIGHT	passenger alighting count
	C_LOAD	updated passenger load now
	STOP_SEQUENCE_ORDER	stop sequence order along a trip
	SCHED_TIME	whether a stop is a time point or not
DIM_STOP	STOPSK	stop ID
	SITE_LONGITUDE	Latitude of the stop
	SITE_LATITUDE	Longitude of the stop
DIM_TRIP_TM	ROUTE_TYPE	route type
	LINE_ID	route ID
	LINE_DIRECTION	route direction
	BLOCK_NUMBER	block ID

In addition to the AVL and APC data, we obtained route segment data containing each route segment's geometry from Metro Transit during the study period. We used the route segment lengths to calculate bus speeds and used their geometries to visualize analysis results. We referred to these route segments as SEG in our later discussion.

We joined the AVL, APC, and route segment datasets and created a master dataset to calculate segment travel time and reliability metrics via the following steps:

- We grouped AVL records into trips based on fields CALENDAR_DATE, BLOCK_ABBR, and TRIP_ID. For each group, we sorted the records by field BLOCK_STOP_ORDER. We created two new columns to store the following stop ID and the actual arrival time at that stop and processed the AVL dataset to get the following stop information. Note that the last stop of a trip did not have the following stop information.
- We joined the AVL and APC datasets based on their shared fields for the calendar date, route ID, block ID, trip ID, and (origin) stop ID. Each stop along a trip had recorded boarding and alighting counts (if any) and the passenger load along the following route segment.
- We then joined the joint AVL-APC dataset and SEG datasets based on the origin and destination stop IDs, the block ID, and the valid date period of each route segment. The joint dataset contained each route segment’s geometry, which overlapped with other datasets and retrieved operating and other environments along each route segment in the following subsection.

3.3.2 Segment Properties

Table 3.3 presents summary statistics of the variables to be used as input variables for our model. The variables were organized into four essential parts: 1) transit service characteristics, 2) the presence of various transit right-of-way, 3) other operating environments along route segments, and 4) nearby land use and population characteristics. We summarized the integration procedures and methods below:

- **Service characteristics** are derived using the route segment features and AVL stop-crossing data.
  - The *route class* was directly retrieved from AVL data.
  - The *segment length* was directly retrieved from the route segment feature's geometry.
  - The *daily trip count* along each segment was calculated by dividing the total number of recorded trips by the total number of days with trips recorded.
  - We also calculated the *percentage of trips during morning and afternoon peak hours* (6:00 AM to 9:00 AM and 3:00 PM to 6:30 PM, respectively).

- **Traffic conditions** for general traffic were obtained from StreetLight during the study period.
  - For *median speed*, *free flow speed*, and *traffic volume* along each route segment, we used the route segment features as the input network links to retrieve these properties directly.
  - For *pedestrian and bicycling traffic*, the buffer areas around road intersections were used as the input to retrieve the volumes. The intersections were then map-matched to route segments to get the total pedestrian and bicycling volume along each route segment.
  - We also used the AADT data provided by MnDOT to get *traffic volumes* (both buses and general traffic) along streets intersecting each route segment.

- **Operating environments** are derived by overlaying route segment features with several datasets:
  - We overlayed the route segments with Minneapolis and Saint Paul downtown boundaries to determine *whether a route segment passed downtown areas*. We also overlayed segments with the University of Minnesota Twin Cities – Twin Cities campus, considering the similar pedestrian and built environments around campus as in downtown areas.
  - We map-matched each route segment with road centerlines to get (1) the percentage along the *freeway*, (2) the percentage along *primary roads*, (3) *the number of road intersections* along the route segment, and (4) the *speed limits* (length-weighted average) along each route segments.
  - We map-matched each route segment with traffic signals from OpenStreetMap and counted the number of *traffic signals per 100 meters* along each route segment.
  - We map-matched each route segment with the buffered area of parking meters along streets and calculated the *percentage of segments with adjacent parking meters*.

- We used the number of through-traffic lanes and the width of each road segment to calculate the *average lane width* along local streets, arterial roads, and highways. Then, we map-matched each route segment with road segments and obtained the *length-weighted average lane width* along each route segment.
- We map-matched route segments with transit advantage lines to get the *percentage (in length) of each segment with transit ROW* of a specific type. The three types were: 1) busways and bus lanes, 2) HOT and HOV, and 3) shoulder lanes.

- **Land use features** are derived by overlaying the route segments with the census block groups used by EPA data and calculating the length-weighted sum of each indicator. We included four indicators with potential impacts on service reliability, including 1) *mixed employment*, 2) *population density*, 3) *pedestrian intersections*, and 4) *network density*.

Table 3.3 frequently used reliability measures (modified from Danaher et al. 2020)

Variable	Description	Mean	Median	Std dev.
Service Characteristics				
Route class (categorical)	Route classification per the Metropolitan Council's Transportation Policy Plan (TPP)			Urban Local – 57.8% Suburban Local – 23.6% Commuter Express – 17.3% Bus Rapid Transit – 1.3%
Segment length	Length of the route segment (in meters)	345.7	223.5	625.2
Daily trip count	Average number of trips per day along the route segment	24.3	19.4	21.0
Ratio of trips in AM and PM peak	Percentage of daily trips during morning and afternoon peak hours (6:00 AM to 9:00 AM; 3:00 PM to 6:30 PM)	4.2	3.7	3.1
Traffic Conditions				
Median speed - all	Median travel speed for all vehicles (mph)	27.9	28.0	9.5
Free flow speed	Free flow travel speed for all vehicles (mph) refined based on speed limits along street segments	30.2	30.0	8.5
Traffic volume	Vehicle counts per 100 meters along the route segment	1571.7	1145.2	1637.7
Average AADT	Average AADT along roads intersecting the route segment	8234.3	6359.0	7980.7
Bicycle and Pedestrian volume	Bicycle and pedestrian volumes along the route segment	1131.8	522.5	2194.8
Operating Environments				
Segment in downtown	Whether the route segment passes the Minneapolis or Saint Paul downtown areas (or the UMN TC campus)			Yes (1) – 11.03% No (0) – 87.97%
Ratio of freeway and ramp	Percentage of the route segment that is along freeways and ramps (no mixed traffic, traffic lights at ramps only)	1.8%	0%	12.5%
Ratio of primary roads	Percentage of the route segment that is operated along primary roads (no mixed traffic, often with traffic lights)	4.1%	0%	19.2%
Ratio of busways and bus lanes	Percentage of the route segment that is operated along bus lanes and busways (transit advantages type)	2.0%	0%	13.2%
Ratio of HOT and HOV	Percentage of the route segment that is operated along HOV lanes and HOT lanes (transit advantage type)	0.2%	0%	4.5%
Ratio of shoulder lanes	Percentage of the route segment that is operated along shoulder lanes (transit advantages type)	2.0%	0%	12.9%
Number of signals	Number of traffic signals per 100 meters along the route segment	0.21	0.37	0
Ratio of parking meters	Percentage of the route segment (length) with designated parking spaces	5.7%	0%	20.2%
Lane width	Average width of lanes in feet	15.5	13.6	5.2
Land Use Features				
Mixed employment	The mix of employment types near the route segment (higher values, more walk trips)	0.6	0.6	0.2
Population density	Gross population density (count per acre) near the route segment	13.6	8.9	41.9
Pedestrian intersections	Pedestrian-oriented intersections near the route segment	116.0	102.1	71.6
Network density	Total road network density near the route segment	23.56	22.94	7.67

3.4 Reliability Calculation

This section presents the methods to calculate travel time and evaluate running time variability for each route segment. Figure 3.2 illustrates the bus movement along a route segment between two stop zones, which includes entering the stop zone, moving to the stop, opening the door for passenger boarding and alighting, closing the door, and waiting if needed to avoid early departure. The stop zone referred to the region 200 feet before and 150 feet past the stop location.

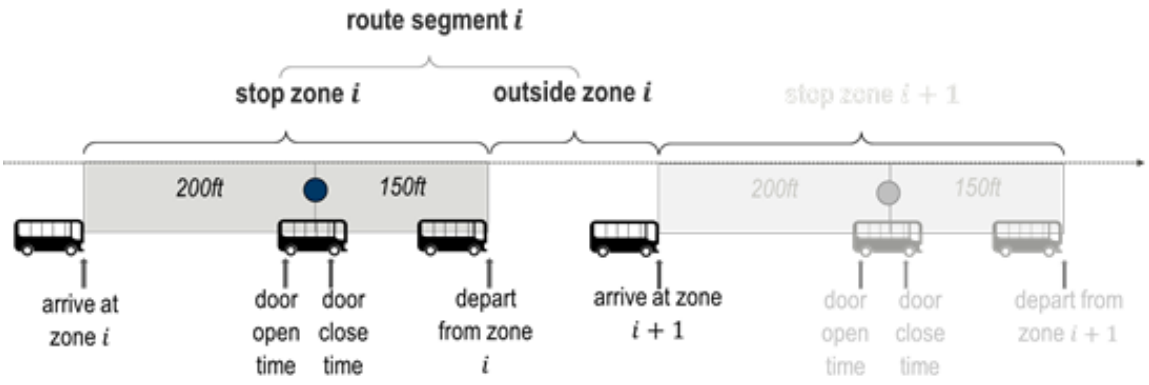

Figure 3.2 Stop zones and breakdown of travel times along a route segment between two stop zones.

We defined the route segment i as the segment along a trip on a route between the entry location of the stop zone i and the entry location of the next stop zone $i+1$. We calculated the travel time of the segment i along trip j of route r following the steps below:

(1) We calculated the total time within the stop zone $t_{i,j}^{z}$ based on the actual arrival time at the zone $t_{i,j}^{actDep}$ and the actual departure time from the zone $t_{i,j}^{actArr}$:

$$t_{i,j}^{z} = t_{i,j}^{actDep} - t_{i,j}^{actArr} \quad (1)$$

(2) We calculated the travel time across the outside the stop zone $t_{i,j}^{o}$ based on the actual departure time from the stop zone $t_{i,j}^{actDep}$ and the actual arrival time at the next stop zone $t_{i+1,j}^{actArr}$:

$$t_{i,j}^{o} = t_{i+1,j}^{actArr} - t_{i,j}^{actDep} \quad (2)$$

(3) We calculated the dwelling time, if any, for passenger boarding and alighting $t_{i,j}^{d}$ based on the first door opening time $t_{i,j}^{doorOpen}$ and the last door closing time $t_{i,j}^{doorClose}$

$$t_{i,j}^{d} = \begin{cases} t_{i,j}^{doorOpen} - t_{i,j}^{doorClose}, & t_{i,j}^{doorOpen} \text{ and } t_{i,j}^{doorClose} \text{ are not NULL} \\ 0, & \text{otherwise} \end{cases} \quad (3)$$

(4) We calculated the potential holding time to avoid early departure for each time point. Specifically, if the bus arrived more than one minute early at a time point, the bus needed to wait at the stop and

left no more than 1 minute earlier than the scheduled time (see Metro Transit's standard for early departure). We referred to this holding time as schedule adherence dwell $t_{i,j}^{h}$ and estimated it based on the last door closing time and the scheduled departure time

$$t_{i,j}^{h} = \begin{cases} t_{i,j}^{schDep} - t_{i,j}^{doorClose}, & i \in TP \; and \; t_{i,j}^{schDep} - t_{i,j}^{doorClose} > 60 \; sec \\ 0, & otherwise \end{cases} \quad (4)$$

(5) The total moving time along the route segment $t_{i,j}^{m}$ was calculated as the total time spent in the stop zone $t_{i,j}^{z}$ and outside zone $t_{i,j}^{o}$ minus the total dwelling time for the passenger boarding and alighting $t_{i,j}^{d}$ and schedule adherence $t_{i,j}^{h}$:

$$t_{i,j}^{m} = t_{i,j}^{z} + t_{i,j}^{o} - t_{i,j}^{d} - t_{i,j}^{h} \quad (5)$$

(6) Considering the various lengths of route segments $\{d_i\}$, we calculated the normalized travel time as the travel time per 100 meters and used it as the basis to calculate reliability metrics.

$$t_{i,j} = t_{i,j}^{m} \times \frac{100}{d_i} \quad (6)$$

After calculating the normalized travel times along route segments, we noticed abnormal moving time within some stop zones ($t_{i,j}^{z} - t_{i,j}^{d} - t_{i,j}^{h} > 30 \; min$). We found that most of them were for the first route segment of a trip. We further investigated the reasons and found that it is very likely due to the holding time needed to prepare for the next service trip at the first stop. Therefore, the first segment of each trip was excluded from our analysis, except for express buses. We kept the first segment along each trip on commuter express routes because it is often the longest part between suburbs and urban areas, with possible HOT/HOV lanes presented. To mitigate the long dwelling time between service trips, we only used travel times in the outside zone along each route segment to calculate the normalized travel time:

$$t_{i,j} = \begin{cases} (t_{i,j}^{z} + t_{i,j}^{o} - t_{i,j}^{d} - t_{i,j}^{h}) \times \frac{100}{d_i}, & i > 1 \\ t_{i,j}^{o} \times \frac{100}{d_i - 350}, & i = 1 \end{cases} \quad (7)$$

We used the median absolute deviation (MAD) of normalized travel times along each route segment to assess its running time variability. Analytically, it can be calculated as:

$$MAD_i = median\{|t_{i,j} - median\{t_{i,j}\}|\} \quad (8)$$

We chose MAD because it was calculated using the median travel time instead of the average travel time and, therefore, was not sensitive to extremely large values. The $\{MAD_i\}$ was used as the output variable for our model.

We further accounted for daily ridership along each route segment and evaluated the impacts of service unreliability on passengers. We used the median daily passenger load along each route segment derived from the APC as the weight and calculated the user-weighted MAD:

$$uMAD_i = MAD_i \times median\{(\sum_{j \in Date_d} load_{i,j})\} \quad (9)$$

3.5 Model Training and Fine-tuning

To evaluate the impacts of transit ROW on service reliability, we used the gradient-boosting regression model (GBM) to associate various factors along route segments, as listed in Table 3.3, with their output reliability metrics. $\{MAD_i\}$. We chose GBM because it can capture nonlinear relationships between input and output variables, can handle highly correlated input variables, allows for the optimization of various differentiable loss functions, can produce highly robust and interpretable learning outcomes, and can deal with the large volume of input data (Bentéjac, C. et al. 2021, Friedman, Sagi and Rokach 2018). We implemented the GBM using the histogram-based gradient boosting (HGBT) regressor in the Scikit-learn packages (scikit-learn.org). We described the algorithm in Appendix A and summarized the implementation process in this section.

- **Variable Selection**. Although GBM regression can handle non-linear relationships among variables, highly correlated variables would still affect model performance and reliability. Specifically, if two variables are highly correlated, either would likely become the split point (node of the tree). Hence, if a set of variables has correlations higher than 0.6 with each other, we chose one variable from the set and used it as the input feature (Cao et al., 2023).
- **Hyperparameter Tuning**. Besides the learning rate and the maximum interaction count (as discussed in Appendix A), we also considered the early stopping and monotonic constraints during the tuning. For the learning rate, we chose 0.01, 0.02, 0.04, 0.06, 0.08, and 0.1 as suggested for GBM, and we included 0.2 and 0.3 in case our data worked better with higher learning rates. For the maximum number of iterations, we used 600, 800, 1000, 1200, 1400, 1600, 1800, and 2000 as our final set after manually testing a few combinations of parameters. We randomly divided the original dataset into training and testing datasets to find optimal parameters. We set the loss function as the mean square error (MSE) for training and testing datasets.
- **Prediction and Evaluation**. After finding the optimal parameters with the least MSE, we trained the model using the entire dataset and visualized the partial dependencies between each input variable and the outcome. To estimate the potential benefits of implementing dedicated ROW, we use the trained model to predict the reliability (MAD) after adding dedicated ROW along route segments by changing the percentage of bus lanes and busways to 100% for segments along local streets. During this process, the research team used the exploratory data analysis results as references to evaluate the modeling outcomes and made necessary adjustments to the model.

3.6 Result Interpretation

The HGBT regressor can provide two interpretations of the learning outcomes: 1) the rankings of feature importance based on their placements across all trees generated through ensemble learning, and 2) the partial dependency plots that show the linear, monotonic, or more complex relationship between each input feature and the output. Moreover, we also adopted the SHAPE (or Shapley Additive eXplanations) as an Explainable Artificial Intelligence (XAI) method to assist with the result interpretations, which used game theory to estimate each feature's contribution to the model's prediction and produced consistent explanations (Lundberg, 2017).

Chapter 4: Results

This section illustrated visual exploration and statistical modeling results. We first presented the service reliability calculation results and their spatial-temporal patterns. We then discussed the GBM learning outcomes, including parameter selection, optimal parameters, feature importance ranking, and partial dependency of features. Last, we illustrated the model predictions and their potential usage in practice.

4.1 Service Reliability

To ensure the analysis results are valid, we included a series of steps to filter out invalid records. Table 4.1 presents the steps and the percentage of records remaining from the previous step.

Table 4.1 Data filtering procedure to remove invalid or incomplete records

Step	Criteria	% records left
1	Remove repeated records	99.052
2	Remove records with no actual arrival time or actual departure time at the stop or actual arrival time at the next stop	97.294
3	Remove out-of-order records (OO indicator is true)	96.482
4	Remove records for segments without matched geometry	96.450
5	Remove records with time not following the order of actual arrival, first door opening, last door closing, and actual departure	96.309
6	Remove records with segment travel times less or equal to zero	96.308
7	Remove records with speed along the route segment lower than 0 mph or higher than 70 mph	96.242
8	Remove records for first stops along trips that were not commuter express	94.996

We first visualized the median speed and reliability metric (MAD) along all route segments across weeks. As shown in Figure 4.1, 1) segments along the suburban local routes had the highest median speed and lowest MAD; 2) segments along the commuter express routes had the lowest median speed and highest MAD; and 3) segments along the BRT routes had higher median speed and lower MAD than those along the urban local routes.

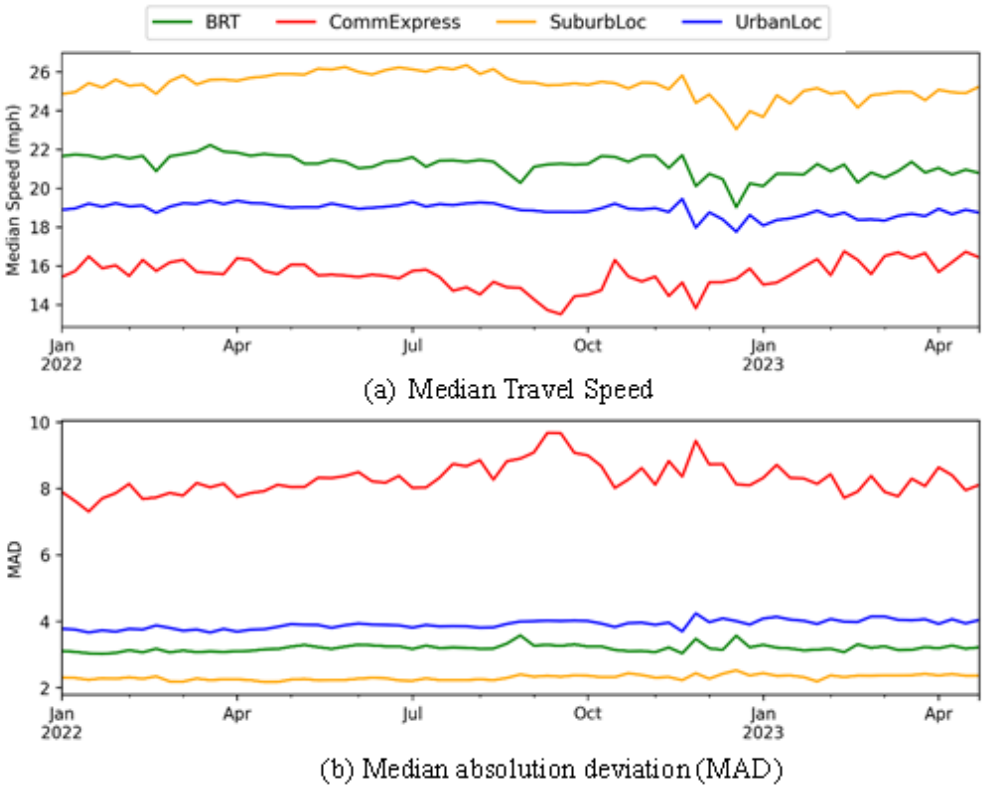

Figure 4.1 Median travel time and MAD across weeks by route service type

We continued to visualize the median travel time and MAD at the route segment level to explore spatial variations of metrics across routes.

- Segments with higher median speeds may have more extensive MAD and less reliable services.
- Suburban local routes generally performed best among all routes. A few routes performed relatively worse than others, including routes 538, 225, 724, 721, and 515.
- Commuter express routes had the most significant variation in median speeds and MAD with a few exceptions: Routes 962, 961, and 967 only provided services during the Minnesota State Fair for 10 days and had the best overall performance among all routes
- BRT routes generally performed better than urban local routes. A few urban local routes have the highest MAD and relatively lower speeds, such as Routes 21, 2, 32, 4, 10, 18, 63, and 74.

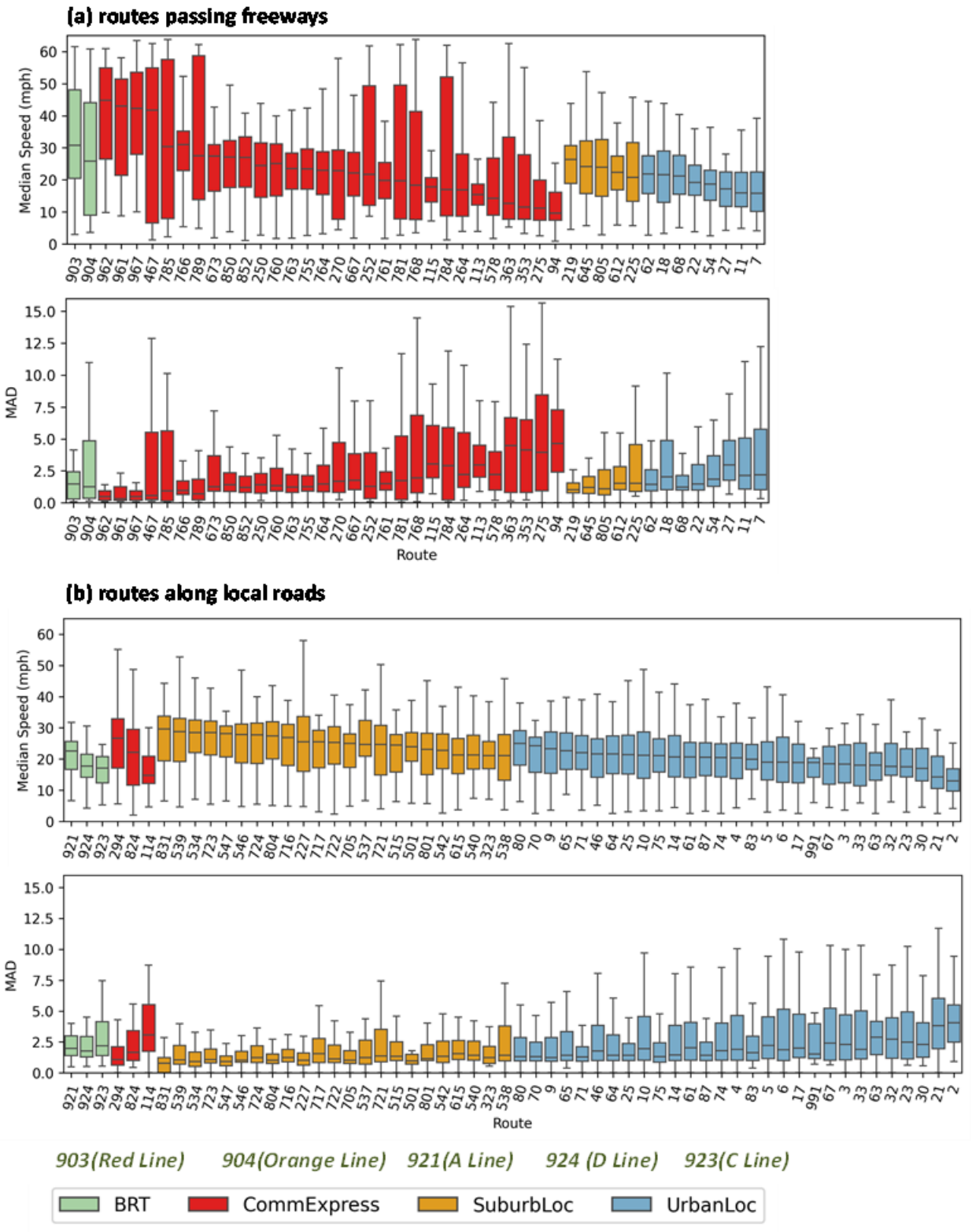

Figure 4.2 Median travel time and MAD along route segments summarized by route

We created an interactive map to explore the spatial variations of median travel time and MAD along route segments. For example, we included the screenshot for MAD along Route 21 East Bound below (see Figure 4.3).

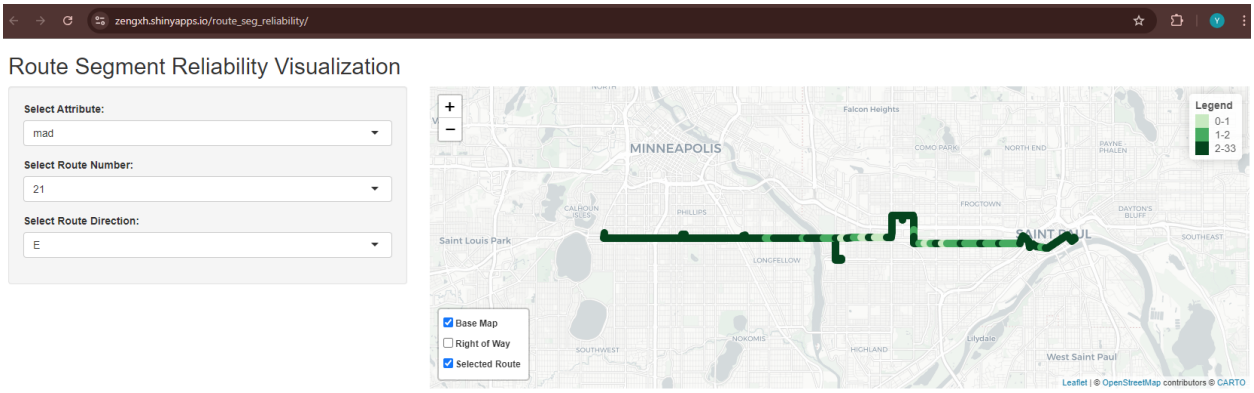

Figure 4.3 MAD for segments along Route 21 East Bound visualized via an interactive online map

In addition to MAD, we also calculated delays at time points (or stops with scheduled departure times) and dwelling times at all stops as two measures from a passenger perspective besides the segment travel times. We examined their variations by developing a dashboard using Streamlit, an open-source Python framework for creating data dashboards. Appendix B describes the dashboard with example analyses.

4.2 Model Parameters

We calculated the Pearson correlation coefficient between all variables in Table 3.1 (see Figure 4.4). If a set of variables has correlations higher than 0.6 with each other, we chose one variable from the set and used it as the input feature for the GBM regressor. For instance, the daily trip counts during all periods, the morning peak hours (AM peak), the afternoon peak hours (PM peak), and the midday were highly correlated, and we chose the daily trip count during all periods as the input feature. For selected variables, we applied the min-max normalization (a.k.a. feature scaling) to rescale each variable to the range of zero to one linearly. The hyperparameter tuning suggested that the model achieved the least MAE of 0.96 using a learning rate of 0.06 and a maximum of 200 iterations.

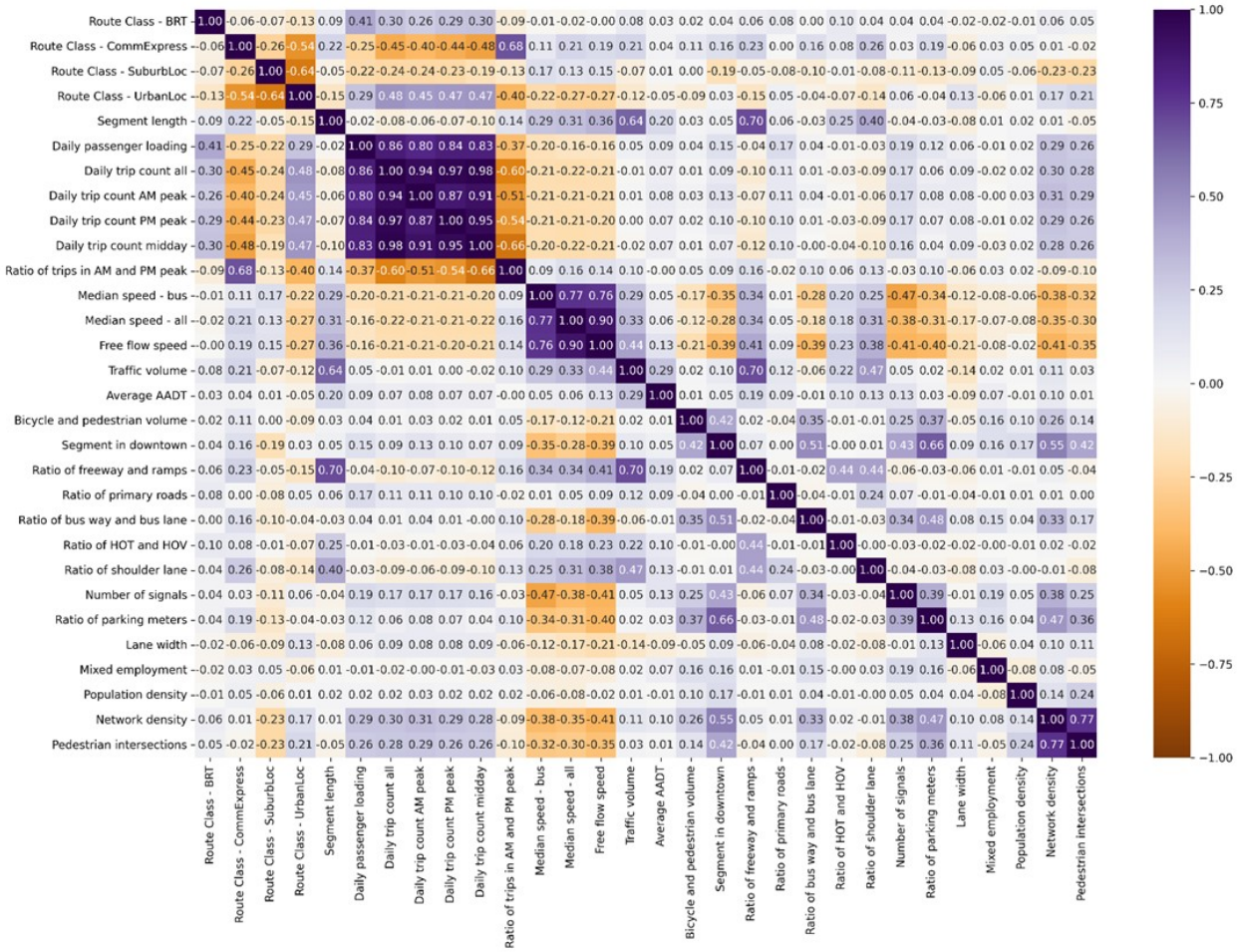

Figure 4.4 Pearson correlation coefficient among all variables

4.3 Feature importance and dependency

Table 4.2 shows the feature importance rankings by the GBM regressor and SHAPE values. Both rankings suggested that the most important features affecting travel time MAD are 1) the free flow speed of traffic, 2) the number of signals, and 3) segment length.

Table 4.2 Rankings of feature importance based on GBM regressor and SHAPE values

Features	GBM Feature Importance	Importance Ranking	SHAPE Values	SHAPE Ranking
Free flow speed	0.443131	1	0.625148	2
Number of signals	0.422902	2	1.094139	1
Segment length	0.168559	3	0.321645	3
Average AADT	0.052565	4	0.145434	4
Daily trip count all	0.044565	5	0.113103	5
Lane width	0.039890	6	0.085590	6
Pedestrian intersections	0.036752	7	0.072685	9
Mixed employment	0.036302	8	0.075666	8
Bicycle and pedestrian volume	0.033059	9	0.070312	10
Ratio of trips in AM and PM peak	0.030067	10	0.080749	7
Ratio of parking meters	0.016416	11	0.043222	11
Ratio of busways and bus lanes	0.004199	12	0.016326	12
Ratio of shoulder lanes	0.002257	13	0.011444	15
Route Class – Urban Local	0.001420	14	0.015096	13
Route Class – Commuter Express	9.51E-04	15	0.004041	16
Route Class – Suburb Local	7.02E-04	16	0.012752	14
Segment in downtown	6.28E-05	17	5.86E-04	17
Ratio of HOT and HOV	1.51E-05	18	5.34E-04	18
Route Class - BRT	0.00	19	0	19

However, the rankings cannot show how each feature contributed to the reliability index MAD. So, we visualized the partial dependencies and SHAPE values. Figure 4.3 presents the SHAPE values for all input features. Each row corresponds to one feature (variable), in which all instances (points) of that feature in the dataset are horizontally distributed along the x-axis based on instances' SHAPE values. A negative SHAPE value toward the left side along the x-axis indicates that the absence of the instance negatively impacts a prediction. The color bar on the right corresponds to the instance values. The instance value appears as a red dot if it is relatively high. If the instance value is relatively low, it appears to be blue. The features are ranked from top to bottom by their mean absolute SHAPE values.

For instance, the free flow speed of general traffic had the highest mean absolute SHAPE values among all features. Higher free flow speeds (red dots) tended to have negative SHAPE values. Lower free flow speeds (blue dots) spread toward a large positive SHAPE value along the x-axis. This suggested that higher free flow speeds were associated with decreased MAD (more reliable services), and lower free flow speeds tended to be associated with higher MAD.

We observed two obvious patterns besides the free flow speed: 1) fewer traffic signals along the route segment were associated with a decrease in MAD, and 2) shorter segment lengths were associated with an increase in MAD. As for various types of transit ROW: 1) a higher ratio of busways and bus lanes was associated with a decrease in MAD, 2) a higher ratio of shoulder lanes was associated with an increase in MAD, and 3) the ratio of HOT and HOV did not have a significant impact on the MAD.

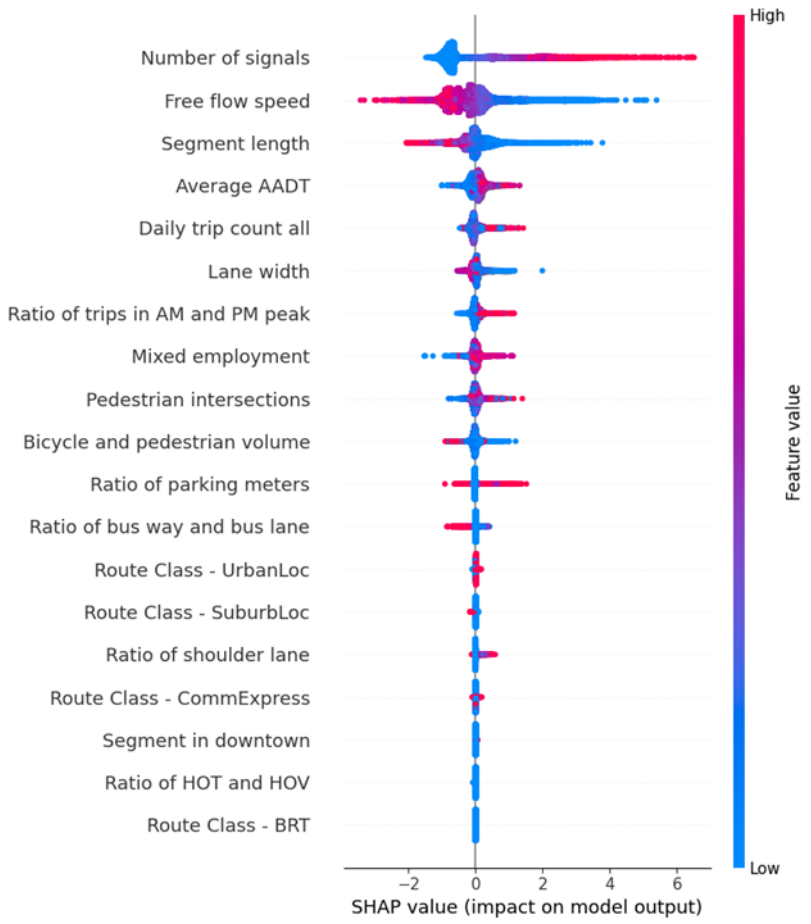

Figure 4.5 Beeswarm plot of SHAPE values for all features

We continued to examine the partial dependencies between input features and the outcome MAD. We visualized partial dependencies for features with interesting patterns in Figure 4.6 and included results for the remaining input features in Appendix C. In each subgraph, the ticks along the x-axis correspond to feature values, and the ticks along the y-axis correspond to positive or negative partial dependencies. The results are consistent with the SHAPE values. As for the three types of transit ROWs:

- An increase in the **percentage of bus lanes or busways** was associated with a decrease in the MAD once such a percentage became larger than 20%. This suggested a positive impact of bus lanes and busways on transit service reliability.
- **The presence of HOT and HOV lanes** was associated with a decreased MAD. However, an increased ratio of HOT and HOV lanes did not further reduce the MAD. Moreover, the absolute importance values remained at less than 0.04. This suggested that buses benefited from HOT and HOV lanes, but the improvement in reliability was subtle.
- **The presence of shoulder lanes** is associated with an increase in MAD. This was likely because buses only utilized shoulder lanes during severe traffic congestion and usually moved at low speeds along these narrow lanes (10 to 12 feet wide). Moreover, those shoulder lanes were typically allocated

along freeways such as I-94 connecting Minneapolis and St. Paul downtown areas, which had high volumes of traffic throughout the entire day. Therefore, the shoulder lanes might help buses avoid extremely long delays but did not help much with common variability measured by MAD.

For the three top contributors,

- Higher **free-flow speeds**, **fewer traffic signals** (per 100 meters), and **longer segment lengths** were associated with decreased MAD and more reliable services.
- This suggested that when designing transit ROWs, it would be wise to
  - ensure a reasonable number of trips along bus lanes and busways to avoid congestion caused by too many buses using a specific bus lane and busway simultaneously and ensure fast, free-flow bus movements along bus lanes and busways.
  - avoid segments shorter than 200 meters with two or more traffic lights. For instance, it might be better to have two consecutive route segments of approximately 200 meters (about one block), each with one traffic light along the path, rather than one longer route segment with two traffic lights and one shorter one with no traffic light.

We also presented the average AADT crossing each route segment and the average lane width along the route segment. The results suggest that

- An increase in the **average AADT** is associated with an increase in MAD, especially when the average AADT is more than 6,000. This was potentially caused by situations when buses are waiting to cross intersections where the traffic lights may prioritize the direction with heavier traffic.
- When the **average lane width** increased from 10 to 18.5 feet, such an increase in lane width was associated with decreased MAD and more reliable service. Such an impact was the most obvious for lane widths from 10 to 12 feet. However, when lanes became wider than 18.5 feet, a wider lane was associated with increased MAD and less reliable service. This suggested that a lane with a width of at least 12 inches can help buses move more smoothly and improve reliability.

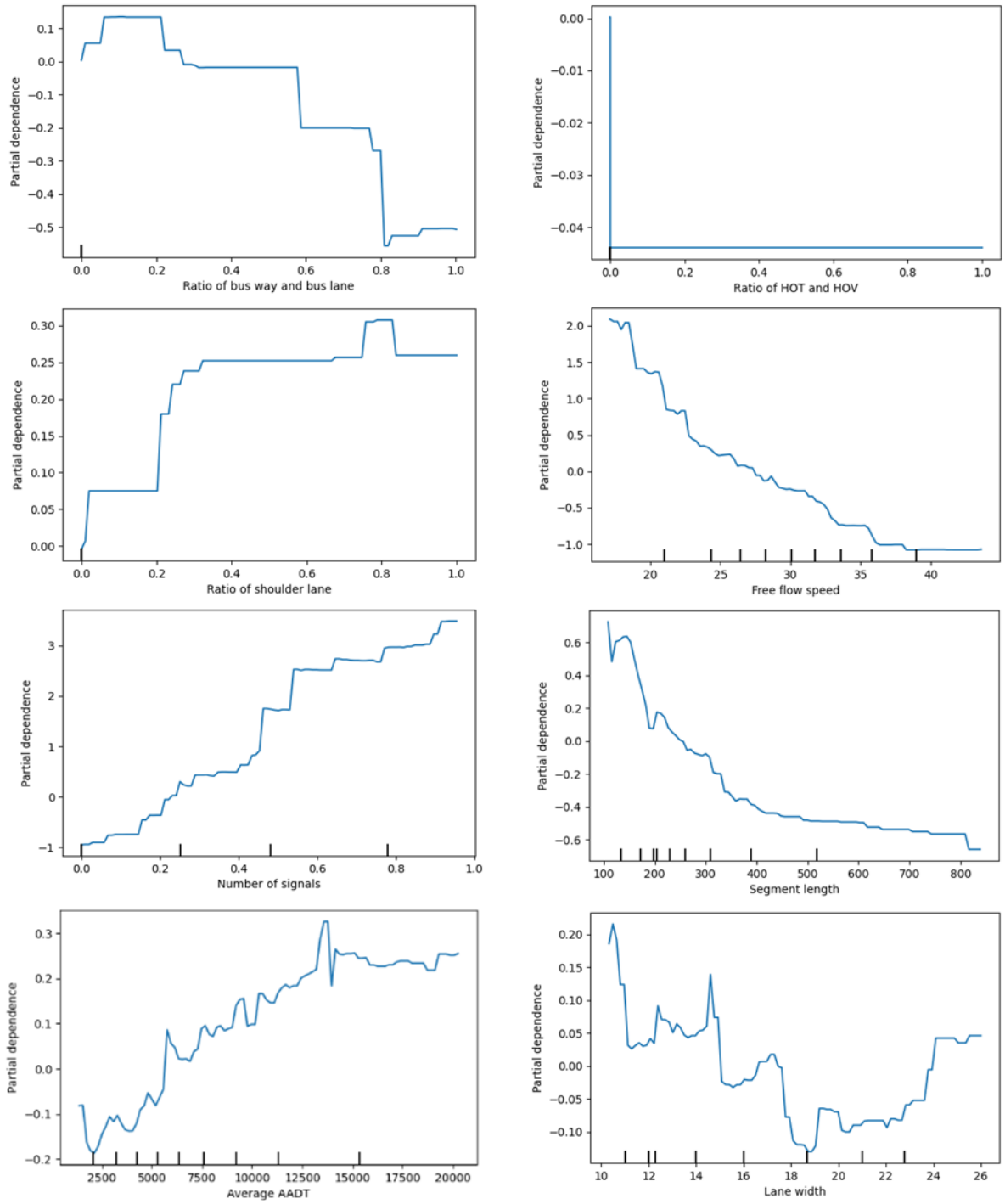

Figure 4.6 Partial dependencies between input features and output MAD

Given the project's focus on the dedicated ROW, we further examined how iterations among features led to the partial dependency between the ratio of busways and bus lanes and the outcome MAD. We used the dependence plot generated by SHAPE and found that the number of traffic signals (per 100

meters) had the strongest interaction with the ratio of bus lanes and busways. Figure 4.7 presents the SHAPE dependence plot. For segments fully operated along busways or bus lanes, most segments had 0.6 or more signals per 100 meters, with a few exceptions below 0.2. Segments with fewer signals were associated with lower shapely values, typically lower than -0.6. These patterns suggested that the ratio of busways and bus lanes interacted with traffic signal density while contributing to the outcome MAD. Hence, it would be essential to account for other factors while evaluating potential improvements in service reliability after implementing a busway or bus lane. For our study case, signal priority could be a great strategy to reduce the negative impacts of traffic signals and further improve service reliability.

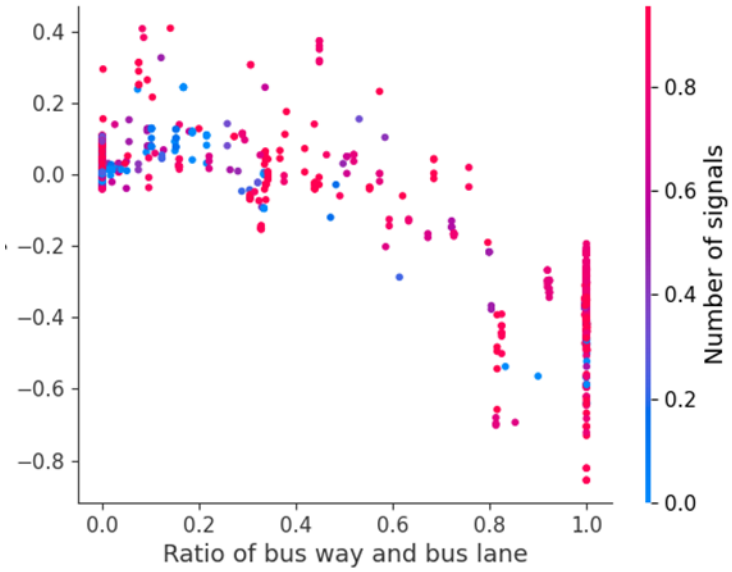

Figure 4.7 Dependency plot for ratio of busways and bus lanes by number of signals

4.4 Values of Dedicated ROW

To evaluate the values of dedicated ROW regarding improved service reliability, we applied the model learned from the entire dataset to estimate the MAD after implementing busways and bus lanes along each route segment. Specifically, we selected route segments that operated along local streets, changed their ratios of busways and bus lanes to 100% and 0%, applied the trained model to estimate the MADs with 100% and 0% bus lanes or busways, and calculated the difference in MADs.

Figure 4.8 presents changes in MAD for all segments. A negative value suggested a decrease in MAD and improved reliability. Route segments in darker green have a higher reduction in MAD. We also included two embedded maps to show changes in the Minneapolis and St. Paul downtown. In general, segments in the Minneapolis and Saint Paul downtown areas and a few transit corridors, such as East Lake Street, may greatly benefit from implementing busways and bus lanes.

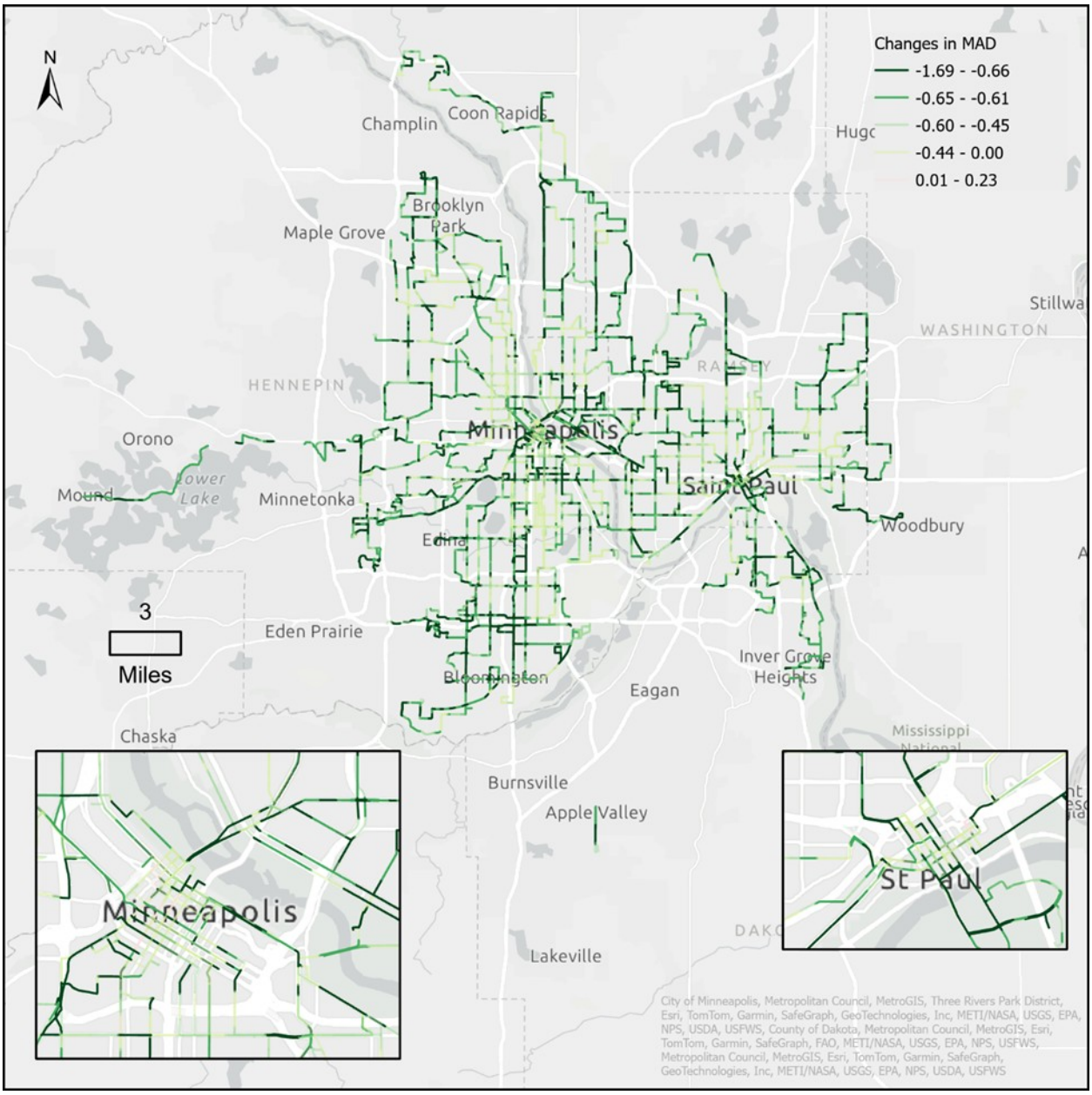

Figure 4.8 Estimated changes in MAD after implementing dedicated ROW along local streets

To highlight the potential benefits of implementing busways and bus lanes along transit corridors with high ridership, we visualized changes in the user-weighted MAD, calculated as the product of MAD and median daily ridership along each route segment. Figure 4.9 presents the results. Segments in darker green had a larger estimated reduction in user-weighted MAD after implementing the busways and bus lanes, which suggested a greater user benefit resulted from improvements in service reliability along these segments.

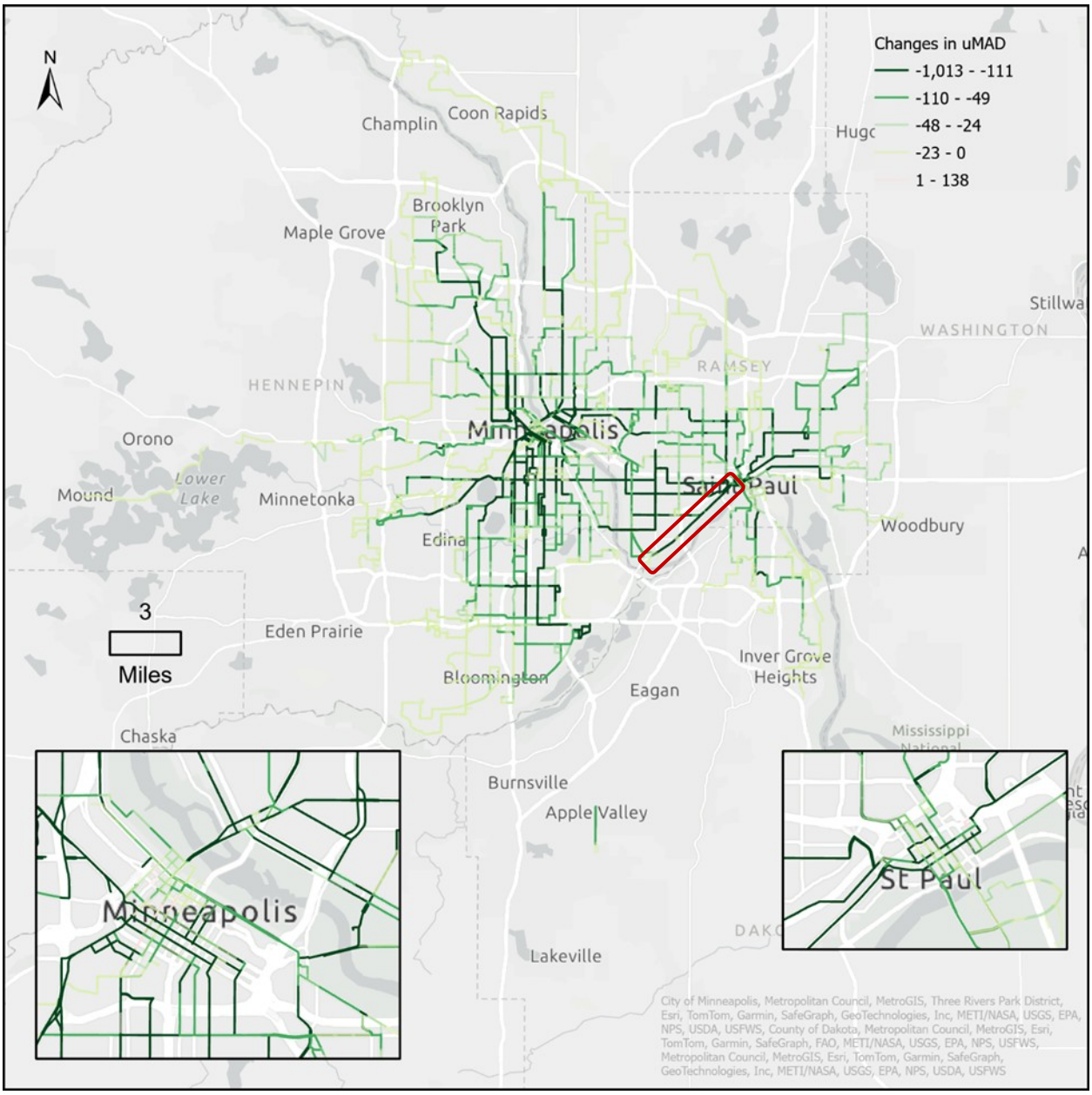

Figure 4.9 Estimated user benefits after implementing dedicated ROW along local streets

Compared to results in Figure 4.8, results in Figure 4.9 further highlight segments that have higher daily ridership and greater user-weighted benefits. For instance, in Minneapolis downtown areas, segments along 7th Street West (highlighted in the red box) do not have the greatest estimated improvement on reliability as shown in Figure 4.8. However, due to the high daily ridership along those segments, they have the largest estimated benefits from implementing bus lanes or busways. These segments are also along the planned Riverview BRT line.

We observed similar patterns in few other service corridors such as segments along East Lake St. and Marshall Ave. toward the South of Minneapolis (along Route 21), along Chicago Ave S. and Portland Ave S. heading toward from downtown Minneapolis (along the southern part of D Line), along Fremont Ave. N. heading north from downtown Minneapolis (along the northern part of D Line), and Central Ave. N. heading north from downtown Minneapolis (along F Line). Combining these findings with segments with the large reduction in MAD (in Figure 4.8), we can identify locations with the most significant reductions in MAD and uMAD. We chose a few examples below to discuss in detail. To help with our discussion, we used images provided by Google Streetview to present operating environments in those selected sites.

- **Route 21:** We started with Route 21 because it had the highest MAD among local routes in our data exploration (see Figure 4.2). As shown in Figure 4.10, reduction in MAD was consistently high along the route, especially at locations where Route 21 intersected with other routes such as 1) BRT A Line at stop 56117 – Snelling and University Station (the right red circle) and 2) Route 7 at stop 53281 – Minnehaha Ave and Lake Street (the middle red circle). Moreover, we observed high reductions in MAD toward the west side of the route (red box on the left), where many routes intersected with Route 21. This suggests that bus lanes can reduce user costs for transferring between these routes.

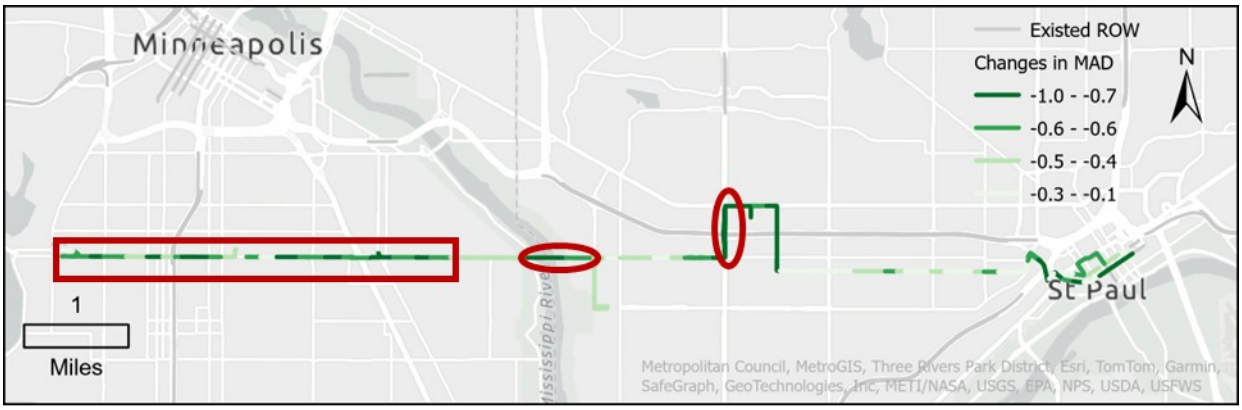

Figure 4.10 Estimated reductions in MAD along Route 21

- **Route 4 and Route 10**: Routes 4 and 10 shared high MAD reductions in the Minneapolis downtown area crossing the bridge along Hennepin Ave (see Figure 4.11). As shown in the Google Streetview image, buses needed to change to the right-turn lane to stop at the bus stop, pick up and drop off passengers, and then merge left back to the straight lane before moving forward to the next stop. Therefore, travel times along segments passing this stop were sensitive to the traffic conditions and likely had large variations. Implementing bus lanes could reduce times spent on changing lanes and the impact of through traffic on bus travel time. Four routes operated along this segment during the study period, all with relatively large reductions in MAD estimated by the trained model.

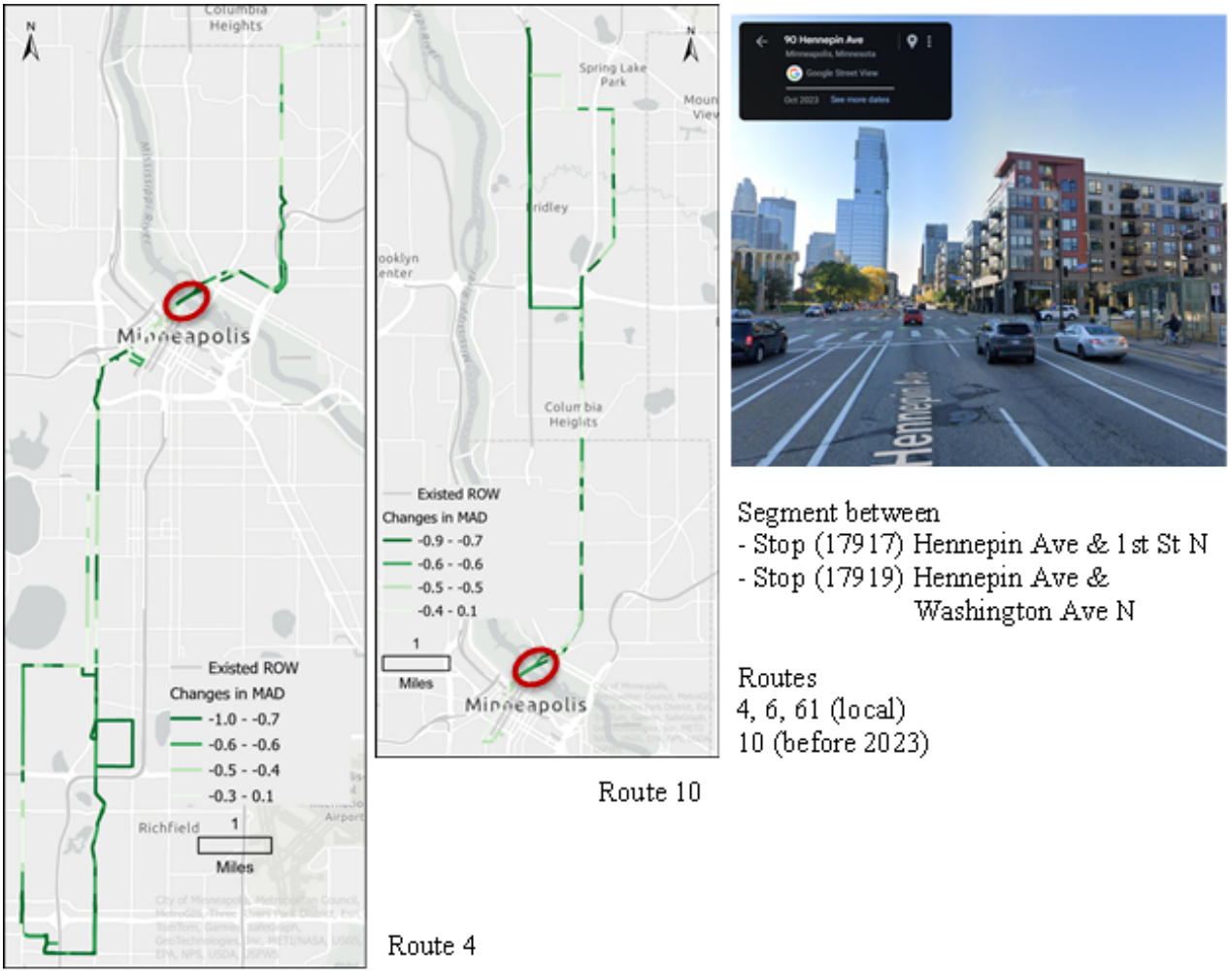

Figure 4.11 Estimated reductions in MAD along Route 4 and Route 10

- **Route 5 and Route 14**: Routes 5 and 14 had high reductions in MAD in the Minneapolis downtown area along South 7th Street and South 8th Street, which were one-way streets serving several local and commuter express routes (see Figure 4.12). This suggests that implementing bus lanes along these segments can bring benefits regarding service reliability and user costs. South 7th Street had bus lanes newly implemented in 2022 (see the Google Streetview image). This was consistent with our findings. Currently, two BRT routes and many local and express routes are utilizing the bus lanes.

The three scenario analyses above showed how the trained models could help us identify locations and service corridors with relatively less reliable services and support informed decisions while planning future dedicated transit ROWs.

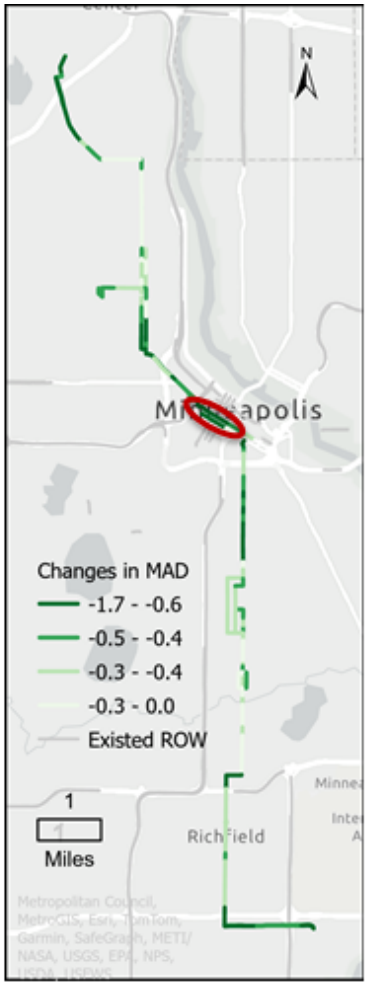

Route 5

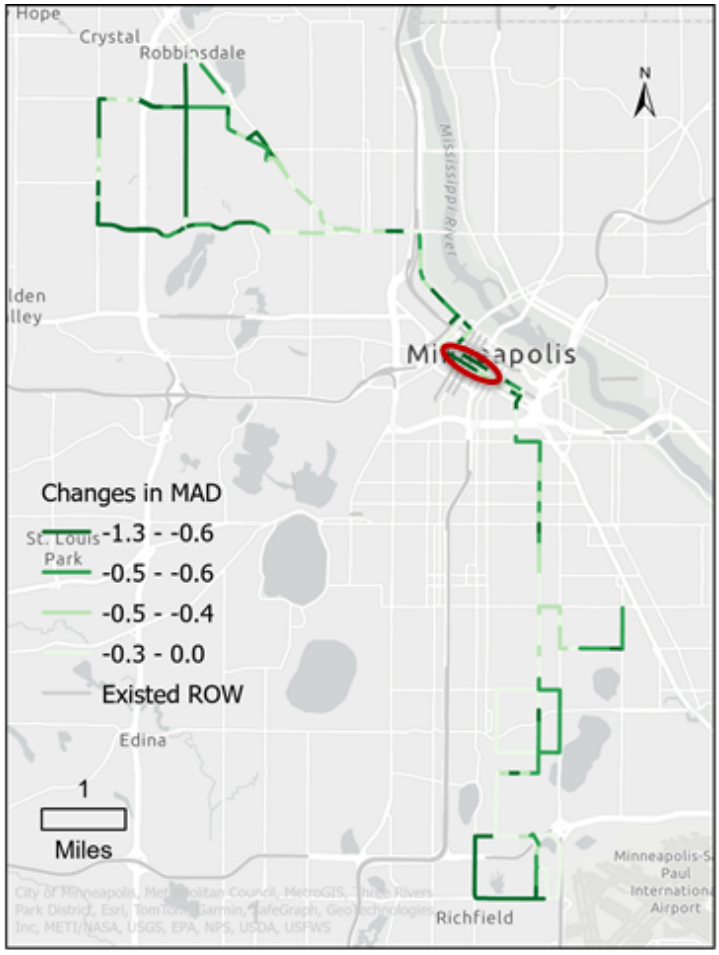

Route 14

Segment along S 7th Street and
S 8th Street in downtown Minneapolis

Routes
C Line, D Line (BRT)
3, 5, 9, 14, 22 …(local)
94, 355, 363, 764, 784,… (express)

Google street view obtained on September 2024 with the newly implemented bus lane along S 7th Street

Figure 4.12 Estimated reductions in MAD along Route 5 and Route 14

Chapter 5: Conclusions

In this research project, we investigated the impact of transit ROWs on service reliability and use costs at the route-segment level in the Twin Cities metropolitan area. Specifically, we collected and integrated AVL, APC, and data from various sources to derive travel time reliability metrics along route segments. We then applied the Gradient Boosting Model (GBM) to uncover the nonlinear relationships between the derived reliability and four types of variables, including service characteristics, traffic conditions, operating environments, and land-use features, with a particular focus on various types of transit ROWs. Lastly, we estimated and compared the travel time reliability with and without the presence of bus lanes and busways for route segments along local streets.

Visual explorations showed differences in travel time reliability across four service types. Suburban local routes generally had the least travel time variability, which was likely due to the relatively light traffic in the suburban areas. Commuter express routes appeared to have the least reliable travel times. This was likely because commuter express trips often operated during morning and afternoon peak hours as well as along popular commuting routes with heavy traffic. Urban local routes and BRT commonly operated in similar environments. Segments along BRT routes along local streets had more reliable services even with more frequent services, which was likely due to signal priority and stop designs along BRT routes.

Results from GBM suggested that three types of transit ROWs had distinct relationships with travel time reliability. Specifically, 1) an increased *ratio of bus lanes and busways* was associated with more reliable travel time only when such a ratio exceeds 20%, 2) the presence of HOV and HOT was associated with higher reliability, but a higher ratio of HOV and HOT did not imply greater improvement, and 3) the presence of shoulder lanes did not help much with reliability. Besides transit ROWs, the model revealed the top-ranking factors associated with more reliable service were 1) higher free-flow traffic speeds, 2) fewer traffic signals, and 3) longer segments. In addition, we found that factors may interact with each other while influencing travel time reliability. This suggested that future design and implementation of dedicated ROWs need to consider other factors, such as signal priority, to maximize their benefits.

Model estimations of reliability revealed route segments along several service corridors that may greatly benefit from bus lanes and busways. Specifically, we compared MADs and user-weighted MADs for each route segment with and without bus lanes and busways and identified segments with higher reductions in MAD. We then examined other routes operating along or across the same corridor to provide a more comprehensive evaluation of the potential benefits of implementing bus lanes and busways. The results revealed several corridors that have the greatest potential benefits, including segments on 1) Route 21 along Lake Street, 2) Route 4 and Route 10 along Hennepin Ave crossing the bridge, and 3) Route 5 and Route 14 along South 7th Street and South 8th Street.

In sum, the project tackled crucial and timely questions in public transportation studies from different angles by evaluating service reliability at the route segment level, identifying key factors contributing to high reliability, and estimating potential improvements in reliability after implementing a dedicated ROW along each route segment. The outcomes can lead to informed decisions about funding future projects, such as prioritizing and implementing bus lanes along service corridors with high potential benefits.

References

Acton, B., Le, H. T., & Miller, H. J. (2022). Impacts of bus rapid transit (BRT) on residential property values: A comparative analysis of 11 US BRT systems. *Journal of Transport Geography*, *100*, 103324.

American Public Transportation Association (APTA). (2020). Designing bus rapid transit running ways. Retrieved from https://nacto.org/wp-content/uploads/2016/05/2-7_APTA-Designing-Bus-Rapid-Transit-Running-Ways_2010.pdf

Benson, J. L., & Cao, J. (2020). Did the A Line arterial bus rapid transit affect housing values in Ramsey County, MN? *Findings*. https://doi.org/10.32866/001c.16628.

Bentéjac, C., Csörgő, A., & Martínez-Muñoz, G. (2021). A comparative analysis of gradient boosting algorithms. *Artificial Intelligence Review, 54,* 1937–1967.

Berrebi, S. J., Lind, E., Brakewood, C., Erhardt, G., & Watkins, K. (2022). Investigating the ridership impact of new light-rail transit and arterial bus rapid transit lines in the Twin Cities. *Transportation Research Record*, *2676*(7)*,* 03611981221078283.

Cao, J., Tao, T., Johnson, I., & Huang, H. (2023). *The value of dedicated right of way (ROW) to transit ridership and carbon emissions*. Retrieved from https://www.cts.umn.edu/research/project/the-values-of-dedicated-right-of-way-to-transit-ridership-and-carbon-emissions

Casello, J. M., Nour, A., & Hellinga, B. (2009). Quantifying impacts of transit reliability on user costs. *Transportation Research Record*, *2112*(1), 136–141.

City of Minneapolis. (2020). Strategy 2: Increase the speed and reliability of transit. Retrieved from https://go.minneapolismn.gov/final-plan/transit/strategy-2

Danaher, A., Wensley, J., Dunham, A., Orosz, T., Avery, R., Cobb, K., … & McLaughlin, J. (2020). *Minutes matter: A bus transit service reliability guidebook*. Retrieved from https://nap.nationalacademies.org/catalog/25727/minutes-matter-a-bus-transit-service-reliability-guidebook

Farr, D. (2011). *Sustainable urbanism: Urban design with nature*. Hoboken, NJ: John Wiley & Sons.

Friedman, J. H. (2001). Greedy function approximation: A gradient boosting machine. *Annals of Statistics, 29*(5)*,* 1189–1232.

Friedman, J. H. (2002). Stochastic gradient boosting. *Comput. Statistical Data Analysis*, *38,* 367–378

González, F., Valdivieso, V., De Grange, L., & Troncoso, R. (2019). Impact of the dedicated infrastructure on bus service quality: An empirical analysis. *Applied Economics*, *51*(55), 5961–5971.

Guthrie, A., & Fan, Y. (2016). *Job growth impacts of bus rapid transit* (Research Brief). Retrieved from https://www.cts.umn.edu/publications/report/job-growth-impacts-of-bus-rapid-transit-research-brief

Ke, G., Meng, Q., Finley, T., Wang, T., Chen, W., Ma, W., ... & Liu, T. Y. (2017). Lightgbm: A highly efficient gradient boosting decision tree. In *Proceedings of the 31st International Conference on Neural Information Processing Systems (NIPS'17)*. Curran Associates, 3149–3157.

Ko, J., Kim, D., & Etezady, A. (2019). Determinants of bus rapid transit ridership: System-level analysis. *Journal of Urban Planning and Development*, *145*(2), 04019004.

Levinson, H. S., Zimmerman, S., Clinger, J., & Rutherford, H. C. S. (2002). Bus rapid transit: An overview. *Journal of Public Transportation*, *5*(2), 1–30.

Lundberg, S. (2017). A unified approach to interpreting model predictions. arXiv preprint arXiv: 1705.07874.

Othman, K., Shalaby, A., & Abdulhai, B. (2023). Dynamic bus lanes versus exclusive bus lanes: Comprehensive comparative analysis of urban corridor performance. *Transportation Research Record*, *2677*(1), 341–355.

Perk, V. A., Flynn, J. A., & Volinski, J. (2008). *Transit ridership, reliability, and retention* (No. NCTR-776-07). Tampa, FL: National Center for Transit Research.

Sagi, O., & Rokach, L. (2018). Ensemble learning: A survey. *Wiley Interdisciplinary Reviews: Data mining and Knowledge Discovery, 8*(4), e1249.

Sakamoto, K., Abhayantha, C., & Kubota, H. (2007). Effectiveness of bus priority lane as a countermeasure for congestion. *Transportation Research Record*, *2034*(1), 103–111.

Suzuki, H., Cervero, R., & Iuchi, K. (2013). *Transforming cities with transit: Transit and land-use integration for sustainable urban development*. Washington, D.C.: World Bank Publications.

Taylor, B. D., & Fink, C. N. (2003). *The factors influencing transit ridership: A review and analysis of the ridership literature.* Los Angeles, CA: UCLA Institute of Transportation Studies

Tirachini, A., Godachevich, J., Cats, O., Muñoz, J. C., & Soza-Parra, J. (2022). Headway variability in public transport: A review of metrics, determinants, effects for quality of service and control strategies. *Transport Reviews*, *42*(3), 337-361.

Van Lierop, D., Badami, M. G., & El-Geneidy, A. M. (2018). What influences satisfaction and loyalty in public transport? A review of the literature. *Transport Reviews*, *38*(1), 52-72.

Wright, L., & Hook, W. (2007). *Bus rapid transit planning guide*. New York: Institute for Transportation and Development Policy.

Appendix A
Gradient Boosting for Regression

Gradient boosting regression tree methods (GBM) are tree-based ensemble methods that combine multiple inducers, each as a simple regression tree, to achieve better prediction performance. The generic algorithm of gradient boosting methods is shown below.

Initialize $F_0(\mathbf{X}) = \text{argmin}_\rho \sum_{i=1}^{N} \mathcal{L}(y_i, \rho)$

For $m = 1$ **to** M **do**

For $i = 1$ **to** N **do**

Compute the negative gradient

$$\tilde{y}_i = -g_m = -\left[\frac{\partial \mathcal{L}(y_i,\ F(x_i))}{\partial F(x_i)}\right]_{F(\mathbf{X})=F_{m-1}(\mathbf{X})}$$

End For

Compute the paramterized class $h(\mathbf{X};\ \boldsymbol{a}_m)$ **(weak learner) that produce** $\mathbf{h}_m = \{h(\mathbf{X}_i;\ \boldsymbol{a}_m)\}_1^N$ **most highly correlate to** $-g_m \in \mathcal{R}^N$ **over the data distribution**

$$\boldsymbol{a}_m = \text{argmin}_{\boldsymbol{a},\beta} \sum_{i=1}^{N} [\tilde{y}_i - \beta h(\mathbf{X}_i;\ \boldsymbol{a})]^2$$

Compute the gradient descent step size as:

$$\rho_m = \text{argmin}_\rho \sum_{i=1}^{N} \mathcal{L}(y_i, F_{m-1}(\mathbf{X}) + \rho h(\mathbf{X}_i;\ \boldsymbol{a}_m))$$

Update the model as

$$F_m(\mathbf{X}) = F_{m-1}(\mathbf{X}) + \rho_m h(\mathbf{X};\ \boldsymbol{a}_m)$$

End For

Output the final model $F_M(\mathbf{X})$

The generic algorithm can be modified given various differentiable loss functions. $\mathcal{L}(y_i,\ F(\boldsymbol{x}_i))$ and different weak learners $h(\mathbf{X};\ \boldsymbol{a}_m)$. Friedman (2002) developed a modified version using a fixed-size regression tree as the base weak learner for gradient-boosting regression.

$$h\left(\mathbf{X}; \{b_{jm}, \mathcal{R}_{jm}\}_1^J\right) = \sum_{j=1}^{J} b_{jm}\, I(\mathbf{X} \in \mathcal{R}_{jm}) \tag{A1}$$

where J is the number of leaves for each tree; $\{\mathcal{R}_{jm}\}_1^J$ are J disjoint regions that collectively cover the space of all joint values of the predictor variables $\mathbf{X}$, the indicator function $I(\mathbf{X} \in \mathcal{R}_{jm})$ equals to one if its argument is valid and zero otherwise.

The "parameters" of this weak learner in Eq. A1 are the coefficients $\{b_{jm}\}_1^J$ and the boundaries of the region $\{\mathcal{R}_{jm}\}_1^J$ at the mth iteration. These define the splits of the tree at the mth iteration, each of which corresponds to a predictor variable and its variable at the split. Therefore, for a regression tree, the updated descent step size and model can be rewritten as

$$again\rho_{jm} = \text{argmin}_\rho \sum_{i=1}^{N} \mathcal{L}(y_i, F_{m-1}(\mathbf{X}) + \rho I(\mathbf{X} \in \mathcal{R}_{jm})) \tag{A2}$$

$$F_m(\mathbf{X}) = F_{m-1}(\mathbf{X}) + \sum_{j=1}^{J} \rho_{jm}\, I(\mathbf{X} \in \mathcal{R}_{jm}) \tag{A3}$$

where a separate optimal ρ_{jm} for each region $\mathcal{R}_{jm}$ is used, so b_{jm} can be discarded. As shown in such a process, the GBM regression tree adopts the stagewise strategy instead of the stepwise strategy, which updates the model by minimizing the expected value of the loss function at each stage.

Friedman also presents specific algorithms for various loss function $\mathcal{L}(y_i, F(\boldsymbol{x_i}))$ for regression, including the least-squares, lease absolute deviation, and Huber-M loss functions. For instance, the least-squares loss function $\mathcal{L}\big(y_i,\ F(\boldsymbol{x_i})\big) = [y_i - F(\boldsymbol{x_i})]^2/2$, so the negative gradient is

$$\tilde{y}_i = -\left[\frac{\partial \mathcal{L}\big(y_i,\ F(\boldsymbol{x_i})\big)}{\partial F(\boldsymbol{x_i})}\right]_{F(\mathbf{X}) = F_{m-1}(\mathbf{X})} = y_i - F_{m-1}(\boldsymbol{x_i}) \tag{A4}$$

Moreover, Friedman (2002) discusses the regularization methods that aim to avoid "overfitting", that is, reducing the expected loss on the training data beyond some point where the expected loss of the population stops decreasing and often starts increasing. Two standard regulation parameters are (1) the number of components M (a.k.a. the maximum number of iterations) and (2) the number of terms in the expansion places. v (a.k.a. the learning rate). The first one regulates the number of iterations so that the model will not become complex and sensitive to minor fluctuations in data. The latter adopts the shrinkage strategy that restricts the number of components and uses "sparse" approximations to achieve better predictions. Hence, equation A3 can be refined as:

$$F_m(\mathbf{X}) = F_{m-1}(\mathbf{X}) + v \cdot \sum_{j=1}^{J} \rho_{jm}\, I\big(\mathbf{X} \in \mathcal{R}_{jm}\big), v \in (0,1] \tag{A5}$$

There is a tradeoff between these two regulation parameters: decreasing the value of v increases the best value of M. Therefore, the optimal values for these two parameters should be estimated by jointly minimizing a model selection criterion concerning both parameters' values. In general, a lower learning rate $v(v < 0.1)$ with a relatively large M is preferable.

The histogram-based GBM regressors can be orders of magnitude faster than the GBM regressors when the sample size exceeds tens of thousands. These fast estimators create integer-valued bins for each input variable. $\boldsymbol{x_i}$ (typically, 256 bins). Instead of sorting continuous values when finding the splitting point and building the tree, only the bin values are examined. This reduces the number of splitting points to consider and speeds up the learning process for large data.

Appendix B
Transit Reliability Dashboard

We built a dashboard using Streamlit, an open-source Python framework for creating data dashboards (https://streamlit.io/). It leverages Automatic Vehicle Location (AVL) data to calculate and visualize the three reliability metrics regarding punctuality at the stop level, dwelling time within the stop zones, and travel time between the stops. The dashboard included interactive widgets and input fields that allowed transit agencies to select various dates, date ranges, routes, and stops for analysis.

Through this dashboard, we addressed the gap in reliability analysis by providing an easily accessible tool for transit agencies to analyze reliability, offering insights into the system performance that would not have been realized with conventional On-Time Performance (OTP) measures. The visualizations on the dashboard focused on investigating the reliability metrics and their deviations and the variability of such deviations across time, allowing the identification of spatiotemporal patterns – figures B1 to B6 present demo visualization using the developed dashboard.

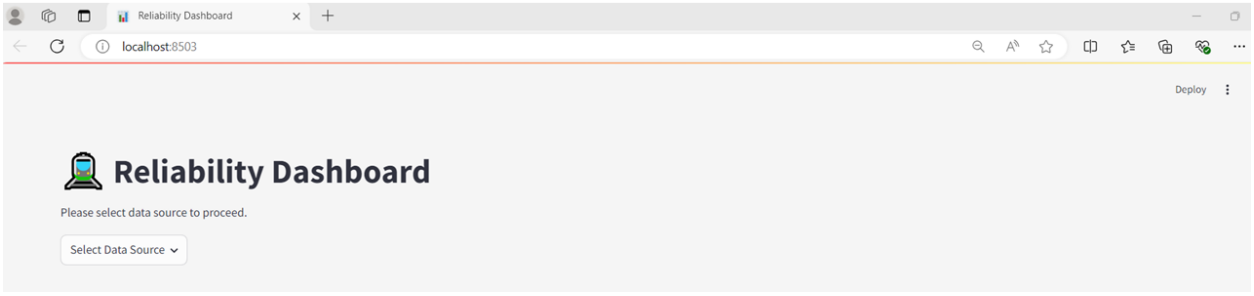

Figure B.1 The opening interface of the reliability dashboard

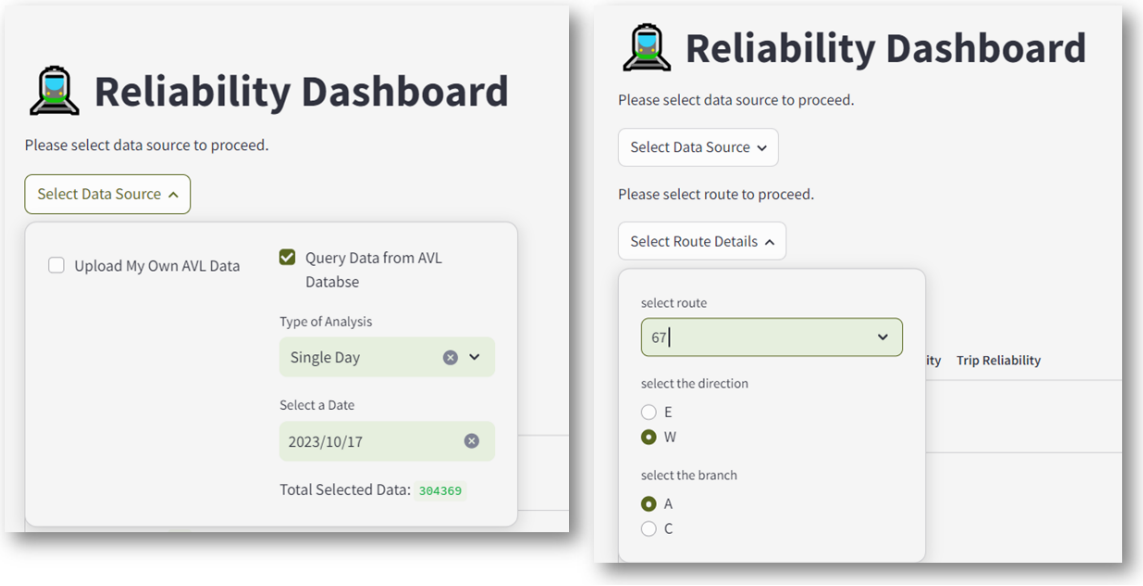

Figure B.2 Input fields for users to select the source of data, type, and date of analysis followed by route selection by direction and branch

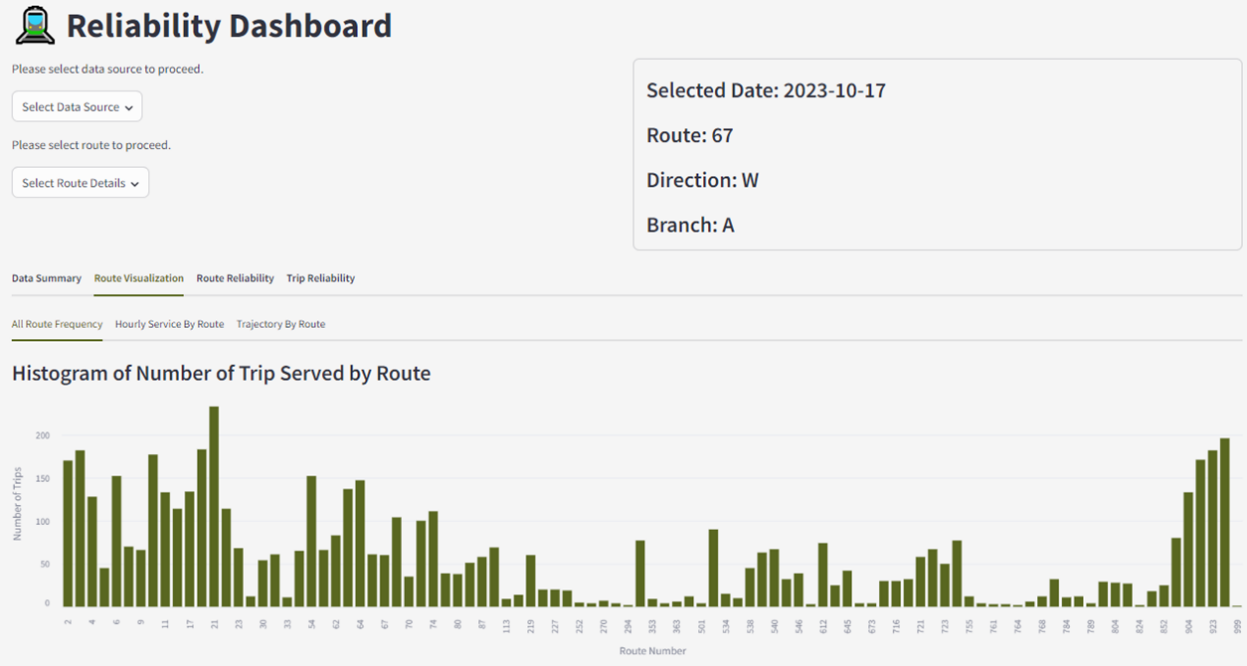

Figure B.3 Multiple analysis tabs enabling users to explore summary data, route visualization, and reliability analysis

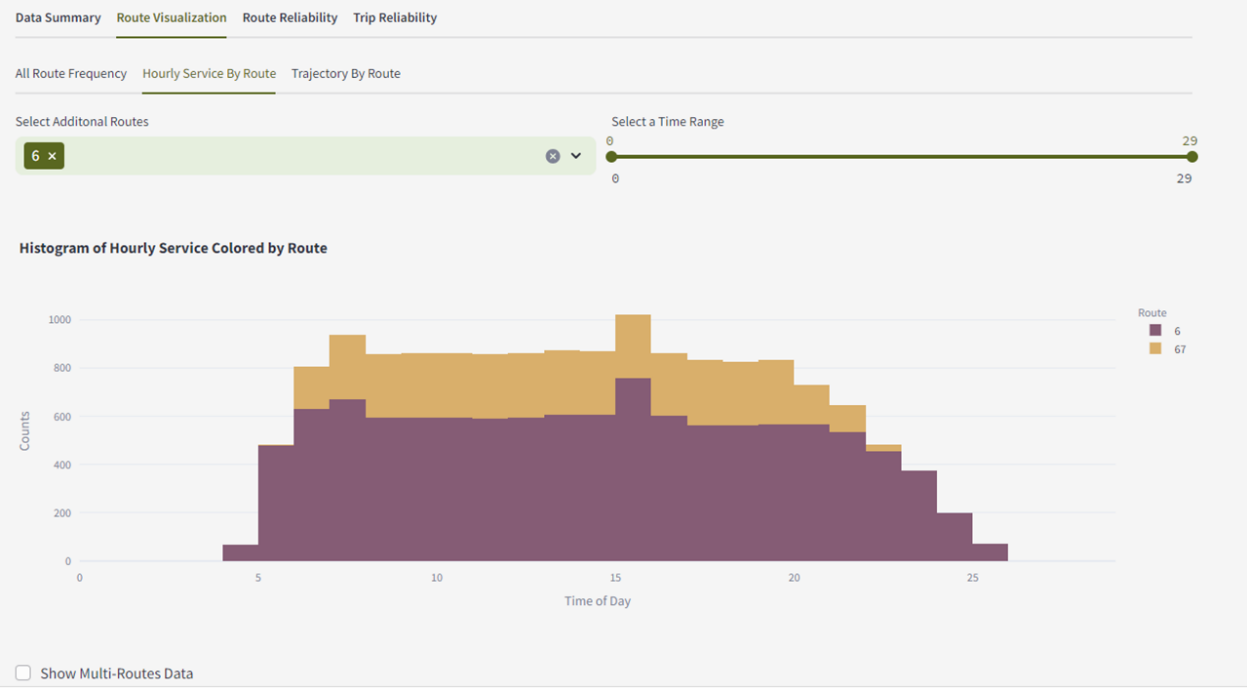

Figure B.4 Route visualization allows the display of multiple routes service (routes 6 and 67) by the hour. options to show selected data are always provided, allowing users to inspect the data further when necessary

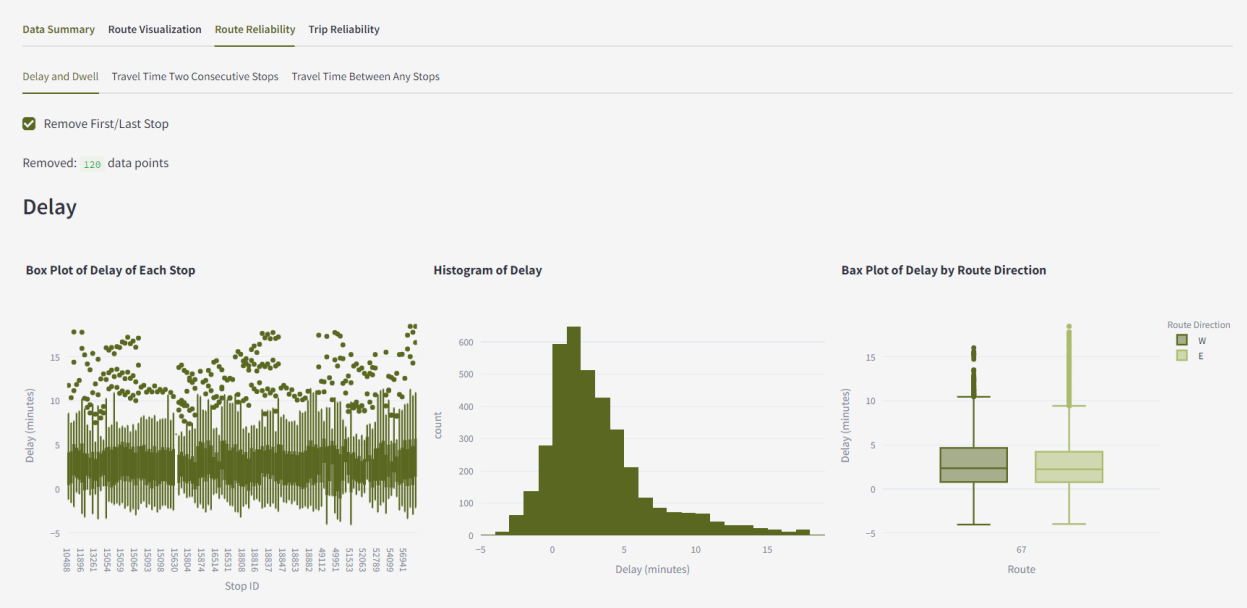

Figure B.5 Reliability analysis can be analyzed at both route- and trip-level (trip-level analysis is under development). Each analysis offers unique insight into the reliability performance. Each plot can be expanded and hovered for detailed information (route 67)

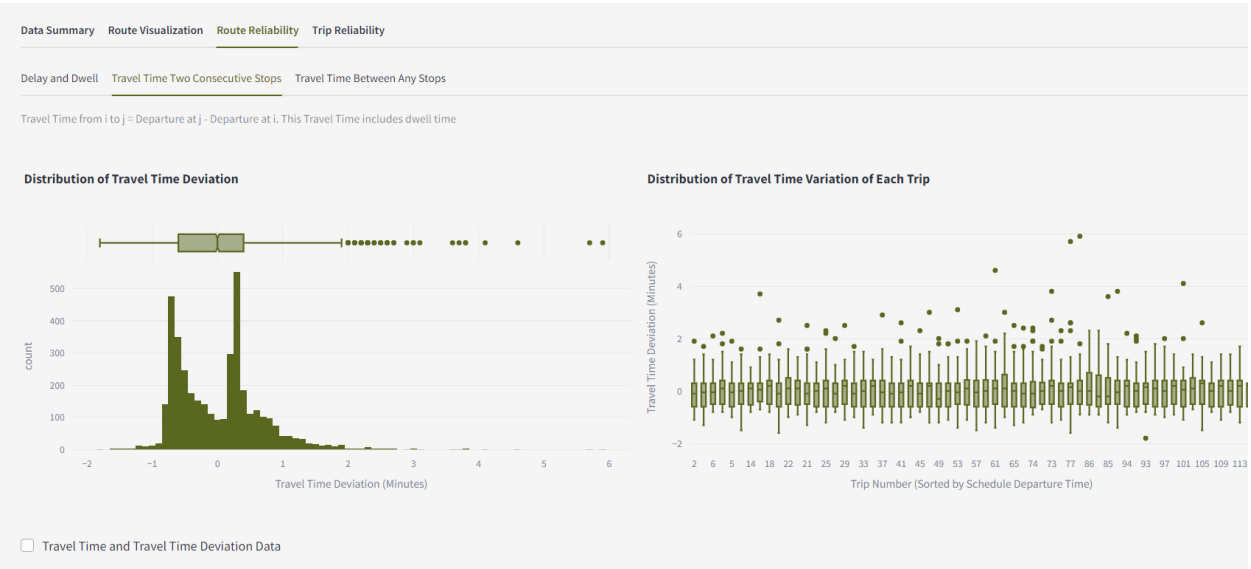

Figure B.6 Travel time between two consecutive stops and between any two stops plotted as a histogram and as a box plot illustrating variation in travel time deviation (route 67)

Figure B.7 Analysis of travel time between any selected stops allows further investigation and gaining better insight into passengers' experience riding between any two stops.

Appendix C
Partial Dependencies of Input Features on MAD

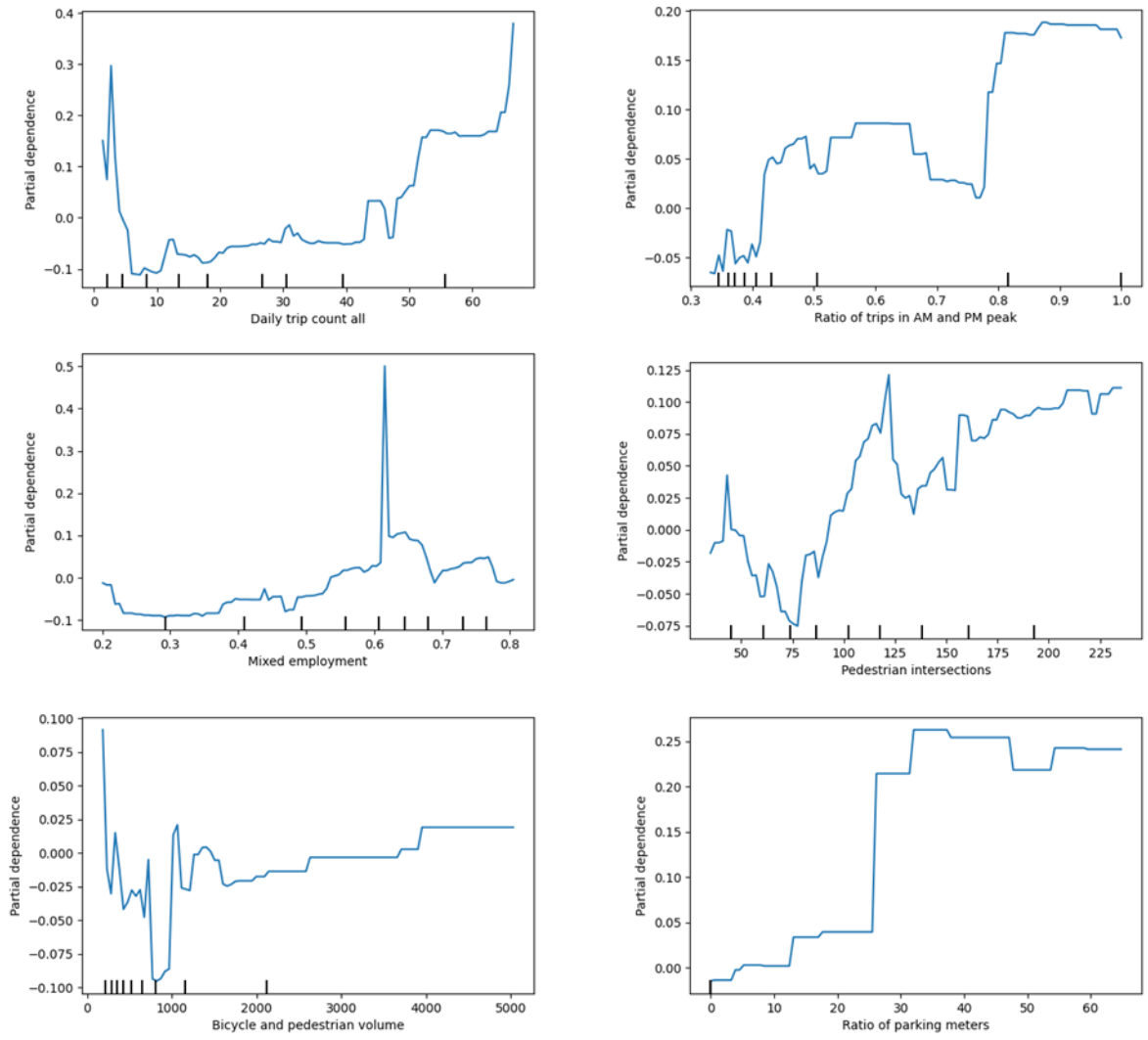

Figure C.1 Partial dependencies between input features and output MAD

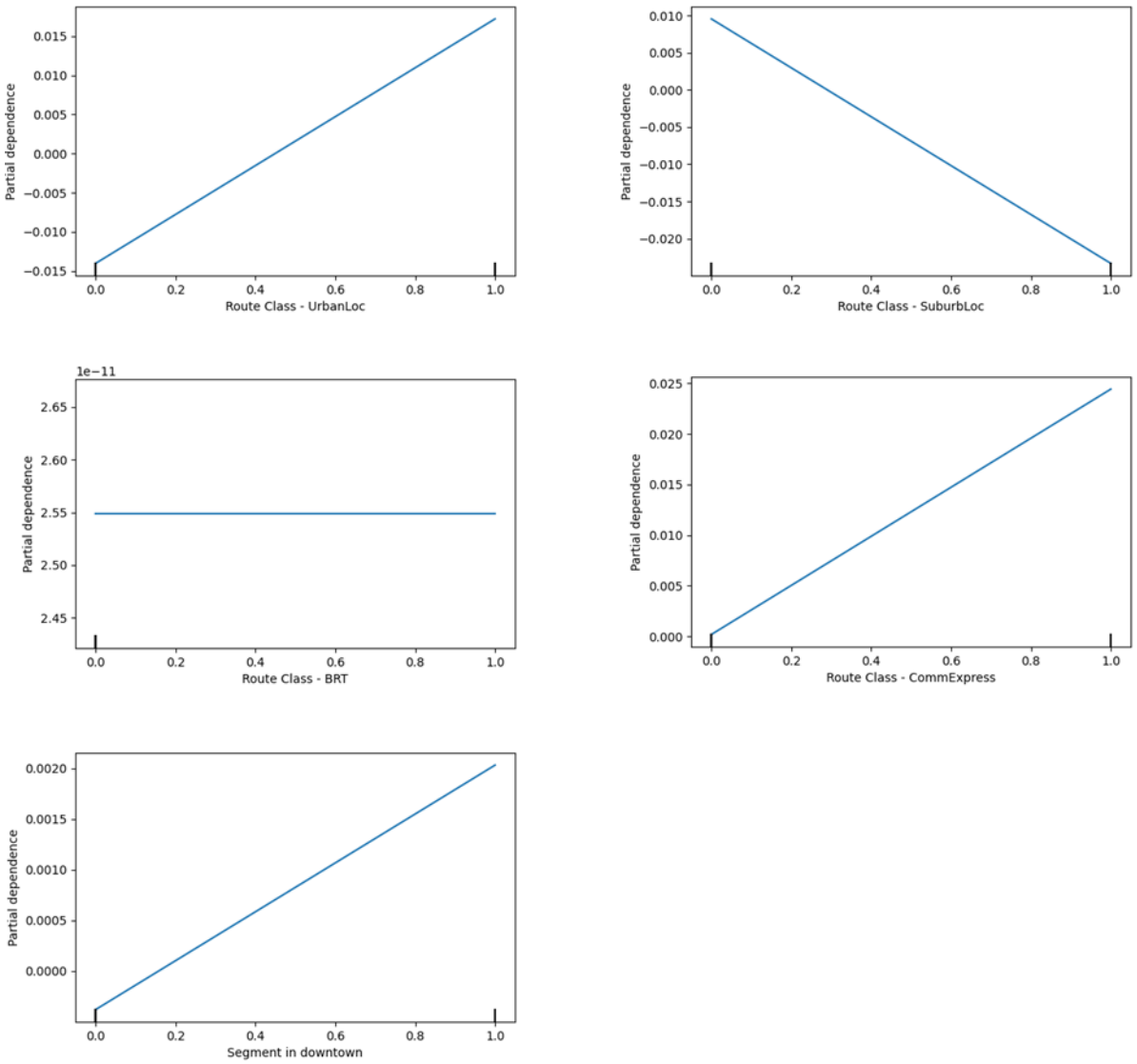

Figure C.2 Partial dependencies between input features and output MAD (continued)